Liquid Crystals
Publication details, including instructions for authors and subscription information:
http://www.informaworld.com/smpp/title~content=t713926090

Invited article Liquid crystal templating of porous materials

Maria E. Raimondi

Online publication date: 06 August 2010

To cite this Article Raimondi, Maria E.(1999) 'Invited article Liquid crystal templating of porous materials', Liquid Crystals, 26: 3, 305 — 339
To link to this Article: DOI: 10.1080/026782999205100
URL: http://dx.doi.org/10.1080/026782999205100

LIQUID CRYSTALS, 1999, VOL. 26, NO. 3, 305–339

Invited article

Liquid crystal templating of porous materials

MARIA E. RAIMONDI and JOHN M. SEDDON*
Department of Chemistry, Imperial College, London SW7 2AY, UK

(*Received 30 June 1998; accepted 18 August 1998*)

1. Introduction

In 1992 Mobil scientists discovered that ionic surfactants could be used as templates for the synthesis of a family of mesoporous siliceous materials which they called M41S. Beck, Kresge and co-workers postulated a 'Liquid Crystal Templating' (LCT) mechanism for the synthesis [1, 2]. Surfactant aggregates similar to lyotropic liquid crystal phases were believed to form within the alkaline colloidal silica synthesis gels, and silicon oxide oligomers polymerized at the surfaces of the amphiphile aggregates forming the porous silica skeleton. The products had a pore size in the mesoscopic range, between 25 and 100 Å, and the pore size distribution was very narrow.

The similarity of these new materials to zeolites was immediately obvious, as were, therefore, the potential applications for mesoporous materials in catalysis and separation technology. An explosion of interest in the field of liquid crystal templating followed as the number of papers published over the past 5 years indicates (see figure 1).

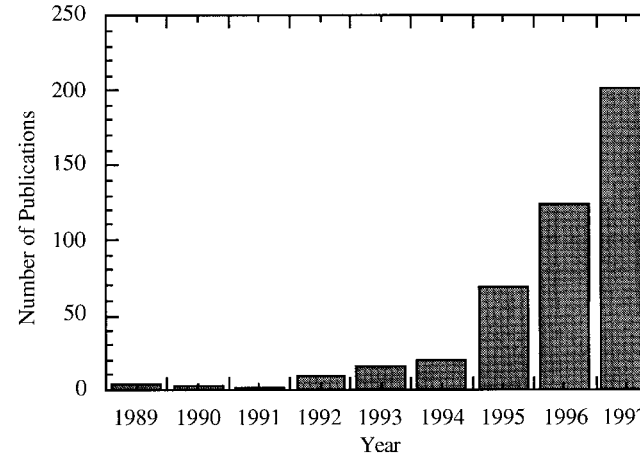

Figure 1. Up-dated plot of the number of papers published in the field of mesoporous materials between 1989 and 1997 (for original plot see the review by T. Maschmeyer [3]). The above data were obtained from a BIDS (Bath Information Data Service) search for the keyword 'mesoporous' in paper titles.

A number of reviews have already been written about liquid crystal templating (LCT) of mesoporous materials and related areas of research [3–16]. In this review we aim to cover all areas of research in LCT, with particular emphasis on mechanistic theories and progress in controlling the synthesis parameters for the production of 'smart' materials.

2. Template theory

Aluminosilicate zeolites have been produced synthetically since the 1950s. In the 1960s tetra-alkylammonium ions were added to zeolite synthesis gels, resulting in the synthesis of new structures such as the ZSM-5 family of zeolites. 'Template Theory' evolved to explain the structure-directing effect of organic species in zeolite synthesis gel [17]. Charge distribution, size and geometric shape of the template molecule were believed to be the main causes of the structure directing process. However, gel chemistry was also crucially important in determining which product was formed. The gel chemistry of the reaction mixture is controlled by factors such as pH, concentration, SiO_2/Al_2O_3 ratio and temperature. The addition of organics affected the gel chemistry of zeolite synthesis mixtures, so it was not clear which factor dominated, template activity or gel chemistry, in determining the product formed.

Many questions remained unanswered about zeolite 'template theory' and until very recently, the discovery of synthetic procedures for making zeolites using organic templates was chiefly by trial and error. However, some progress has now been made in understanding zeolite templating. In particular, computer modelling has been successful in predicting the templates required for certain zeolite syntheses [18–23]. Both known templates and a new one, which was subsequently proven experimentally to direct a certain zeolite structure, were generated by the model. This was an important early step towards the synthetic ideal of 'tailor-made zeolites'.

*Author for correspondence.

Journal of Liquid Crystals ISSN 0267-8292 print/ISSN 1366-5855 online
http://www.tandf.co.uk/JNLS/lct.htm
http://www.taylorandfrancis.com/JNLS/lct.htm

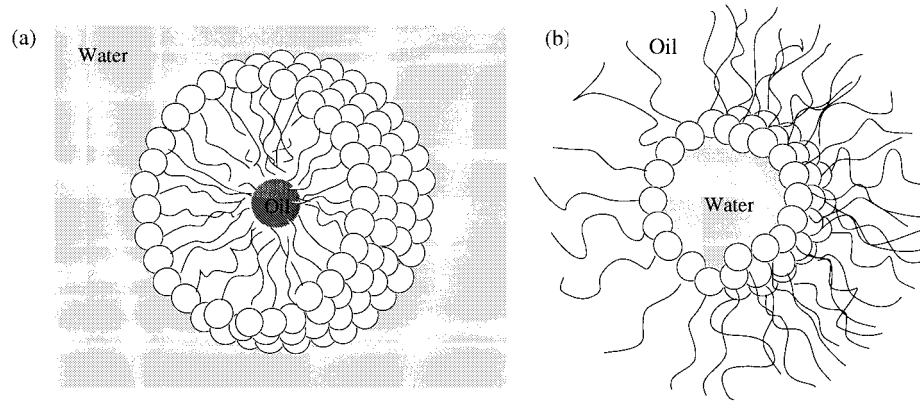

Figure 2. Schematic diagrams of: (*a*), a *normal* micelle; (*b*), an *inverse* micelle.

Zeolites are in general *microporous*, usually with pore sizes smaller than 10 Å. Their very high surface area and small pore size distribution has made them valuable in selective catalysis applications and in separation technology. Zeolites are now of immense importance in industry and are found in everyday household goods such as washing powders and water softeners.

Mesoporous materials, where the pore size can extend to greater than 100 Å, are generally synthesized via a supramolecular templating mechanism. Because of their larger pore size, these materials are not restricted to the catalysis of reactions involving small molecules, as is the case for zeolites. Mesoporous materials have potential catalytic/separation technology applications in the fine chemicals and pharmaceutical industries. The first mesoporous products were pure silicates or aluminosilicates. More recently, the addition of key metallic or molecular species into the siliceous mesoporous framework, and the synthesis of various other transition metal oxide products has extended the applications of these materials to very diverse areas of technology. Potential uses for mesoporous 'smart' materials in sensors, solar cells, nanoelectrodes, optical devices, batteries, fuel cells and electrochromic devices amongst other applications have been suggested in the literature.

3. Supramolecular templating

In liquid crystals, molecules, aggregates of molecules, or macromolecules self organize into phases in which orientational order and/or positional order (in one, two or three dimensions) persist over macroscopic distances. Lyotropic phases are generally obtained by solvating *amphiphilic* molecules, containing both hydrophobic and hydrophilic groups with hydrophilic solvents (often water). Amphiphiles having strongly hydrophilic groups tend to form Type 1 (oil in water) or *normal* phases; those with strongly hydrophobic groups may form Type 2 (water in oil) or *inverse* phases. In the first case, the polar/non-polar interface is curved away from the water, whilst in the second it is curved towards the water (see figure 2). Phase transitions are in part driven by the preferred interfacial mean curvature, which depends on solvent concentration, temperature, pH and other factors [24].

The most familiar lyotropic phases are those obtained on adding surfactants to water. The surfactant molecules undergo reversible self assembly into larger aggregates which in turn self-organize over a larger scale into liquid crystals [25]. In figure 3, L_α stands for the lamellar phase, H_I and H_{II} are the normal and inverse hexagonal phases, a and d are the inverse and normal micellar cubic phases, respectively, and b and c are the inverse and normal bicontinuous cubic phases, respectively.

In LCT theory, lyotropic liquid crystal phases are present in the synthesis gels which mould the resulting porous solid to their own structure. In the original research on mesoporous M41S structures, the aluminosilicate products resembled phases known for lyotropic cetyltrimethylammonium bromide (CTAB) liquid crystals [1] (see figure 4).

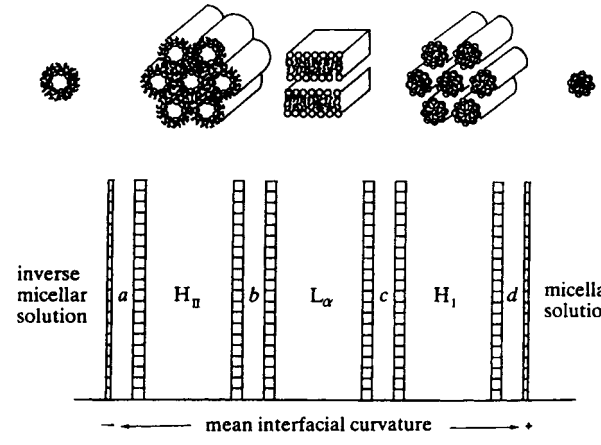

Figure 3. The principal lyotropic liquid crystalline phases arranged according to increasing mean curvature at the polar/non-polar interface [24]. Reprinted with permission from Seddon, J. M. and Templer, R. H., 1993, *Phil. Trans. Roy. Soc. Lond. a*, **344**, 377.

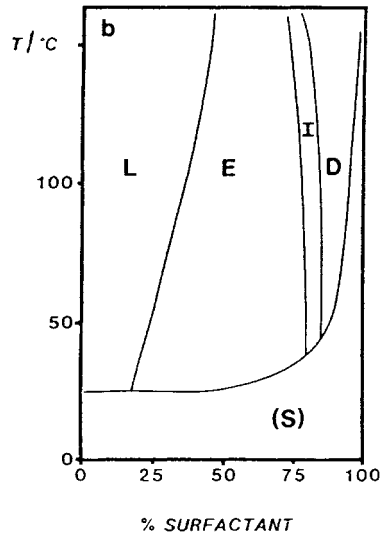

Figure 4. Phase diagram for CTAB in water [26]. E, I and D are hexagonal, cubic and lamellar liquid crystalline phases, respectively. (S) is solid surfactant and L is the solution phase. Reprinted with permission from J. Coll. and Interface Sci., 1988, **125,** 627.

4. Liquid crystal templating in the dilute solution regime: the M41S family

Until the discovery of liquid crystal templating in 1992 [1, 2], synthetic zeolites were mainly microporous. The largest pore sizes obtained for regular, uniform channel solids were approximately 10–12 Å (for metallophosphates) and 14 Å for mineral cacoxenite. Mesoporous solids included silicas and modified layered materials, but these were invariably amorphous or paracrystalline solids, with irregularly spaced pores with broad pore size distributions.

In their papers on LCT, Beck *et al.* [1] and Kresge *et al.* [2, 27] reported the synthesis of mesoporous materials with pore sizes in the range 20 to 100 Å, from aluminosilicate gels containing surfactants. The synthesis gels contained a low concentration of CTAB with respect to that required to form a liquid crystal phase, together with an alkaline colloidal silica precursor. The ordered structure precipitated out of the synthesis mixture after several hours hydrothermal treatment giving a composite silica/organic structured phase. This was then calcined to remove the organic material. The resulting M41S materials contained regular arrays of uniform channels, the dimensions of which could be tailored through the choice of surfactants, auxiliary chemicals and reaction conditions. It was proposed that the formation of these materials took place by means of a LCT/mechanism, in which the silicate material formed inorganic walls between ordered surfactant micelles.

The most studied of these materials was MCM-41 (MCM = 'Mobil composition of matter'), which possessed a hexagonal array of uniform mesopores. In early work the silica source in the alkaline synthesis gel was either colloidal silica, e.g. commercially available 'Hi-Sil' [1] or sodium silicate [28]. Work conducted later led to procedures using tetramethoxysilane (TMOS) or tetraethoxysilane (TEOS) as precursors for the silica, instead of the alkaline colloidal silica. Silicate oligomers were formed by either base- or acid-catalysed hydrolysis of the alkoxysilane, which then condensed into the silica structure [29]. The calcined mesoporous products had Brunauer-Emmett-Teller (BET) surface areas greater than 1000 $m^2\ g^{-1}$, and exceptionally high sorption capacities. Relatively large hexagonal prisms of MCM-41 were obtained which could be seen (figure 5) by scanning electron microscopy (SEM).

The nature of the ordering in the material walls at an atomic level is not fully understood. There were no sharp peaks at wide angles in the powder X-ray diffraction patterns (figure 6) suggesting that there was no ordering at an atomic level. The self-assembled organic–inorganic composites therefore did not contain crystalline inorganic regions. The inorganic portions had only local order (1st and 2nd co-ordination) similar to that of amorphous oxides [1].

The pore diameter in MCM-41 was varied by changing the alkyl chain length of the cationic surfactant templates used in the synthesis procedure. For example, by substituting dodecyltrimethylammonium ions, $C_{12}H_{25}(CH_3)_3N^+$, for hexadecyltrimethylammonium, $C_{16}H_{33}(CH_3)_3N^+$, ions, the resulting molecular sieve had 22 Å diameter pores rather than 37 Å pores. Another method used for altering the pore diameter was to add

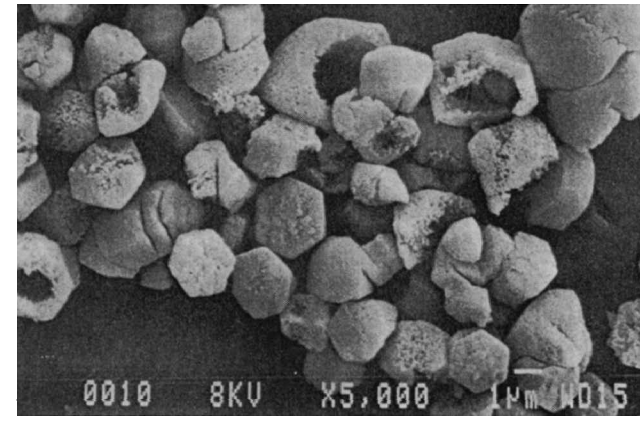

Figure 5. Scanning electron micrograph of an MCM-41 sample. The micrograph was obtained on a JEOL JXA-840 scanning electron microscope using conventional sample preparation and imaging techniques [2]. Reprinted with permission from *Nature*, 1992, **359,** 710. Copyright 1999 Macmillan Magazines Limited.

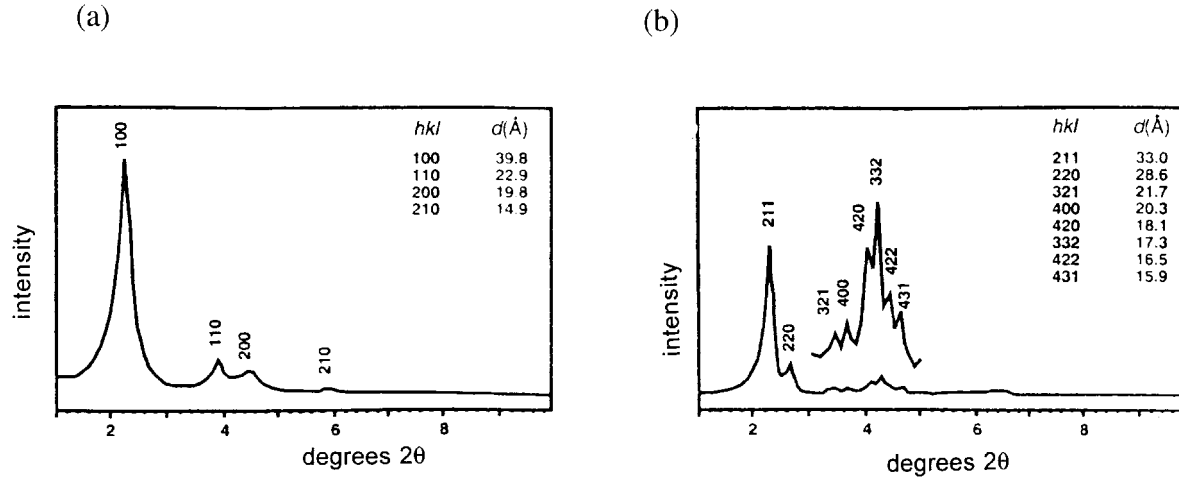

Figure 6. (*a*) Representative X-ray diffraction pattern of MCM-41 (2D-hexagonal symmetry, plane group *p*6*mm*). (*b*) Diffraction pattern obtained for a cubic (*Ia*3*d*) material, MCM-48, also prepared by LCT. Inset is the expansion of the region $2\theta = 3–5°$ [1, 2]. Reprinted with permission from *Nature*, 1992, **359,** 710. Copyright 1999 Macmillan Magazines Limited.

auxiliary hydrocarbons, such as 1,3,5-trimethylbenzene (mesitylene), to the reaction mixture. This resulted in pore sizes as large as 100 Å (see the table, and figure 7).

X-ray diffraction on these solids gave strikingly similar results to the lyotropic liquid crystalline hexagonal phases produced using the alkyltrimethylammonium surfactant/water mixtures at specific amphiphile concentrations. The H_I (normal hexagonal) phases of the templates in water had properties which were analogous to those of the MCM-41 synthesis products, suggesting that the H_I phase was directly implicated in the MCM-41 synthesis: the *d*-spacings obtained by X-ray diffraction on the hexagonal liquid crystalline phases depended on the alkyl chain length of the surfactant; organic species could be solubilized inside the hydrophobic regions of the micelles leading to an increase in the micelle diameter (larger *d*-spacings).

Two different possible pathways were initially suggested for the formation of the liquid crystal templated material:

(1) The liquid crystal phase was intact before the silicate species was added.
(2) Addition of silicate resulted in the ordering of the subsequent silicate-encased surfactant micelles.

These two pathways are depicted in figure 8. In both cases the resultant silicate/surfactant structure mimics known liquid crystal phases. However, due to the low initial surfactant concentration, the second route is the more likely, proceeding via co-precipitation of the organic template with the silica species out of the high water content synthesis gel. The presence and distribution of silanol groups in MCM-41 materials was studied by MAS Si-NMR. Silanols could be expected to

Table. Effect of surfactant chain length on MCM-41 pore size (as determined by Ar adsorption), XRD d_{100} peak location, hexagonal unit cell parameter, a_o, and benzene uptake [1]. Reprinted with permission from *J. Am. chem. Soc.*, 1992, **114,** 10 834. Copyright 1999 American Chemical Society.

Surfactant chain length $C_nH_{2n+1}(CH_3)_3N^+$ $n=$	XRD d_{100} *d*-spacing/Å	a_0/Å[a]	Ar pore size/Å	Total benzene uptake/ wt % at 50 Torr
Siliceous products				
8	27	31	18	16
9	28	32	21	37
10	29	33	22	32
12	29	33	22	36
14	33	38	30	54
16	35	40	37	64
Aluminosilicate products				
12	31	36	—	43
14	34	39	34	40
16	39	45	38	61

[a] $a_0 = 2d_{100}/\sqrt{3}$.

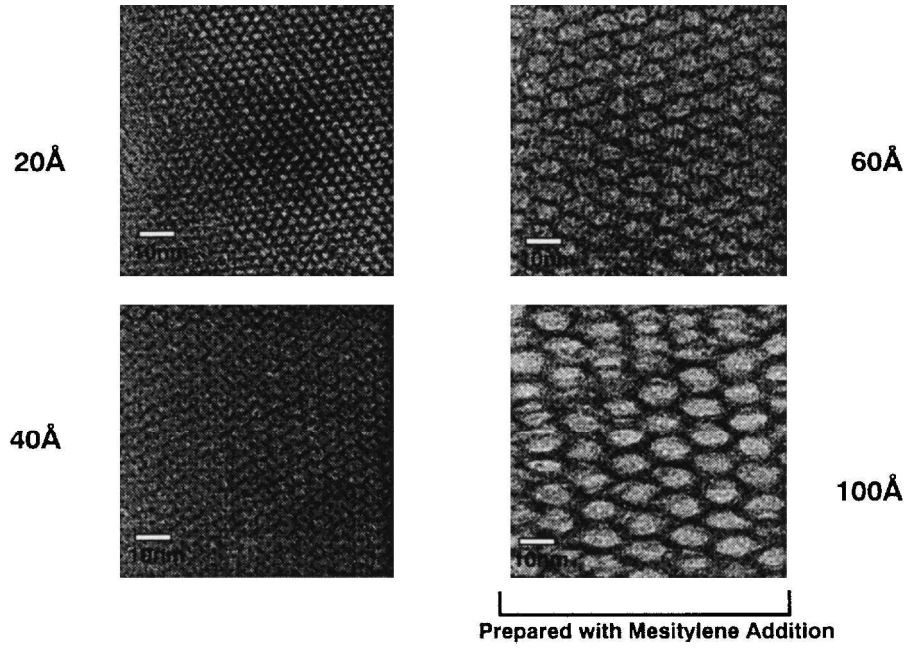

Figure 7. Transmission electron micrographs of selected MCM-41 materials having 20, 40, 60 and 100 Å pore channels [4].

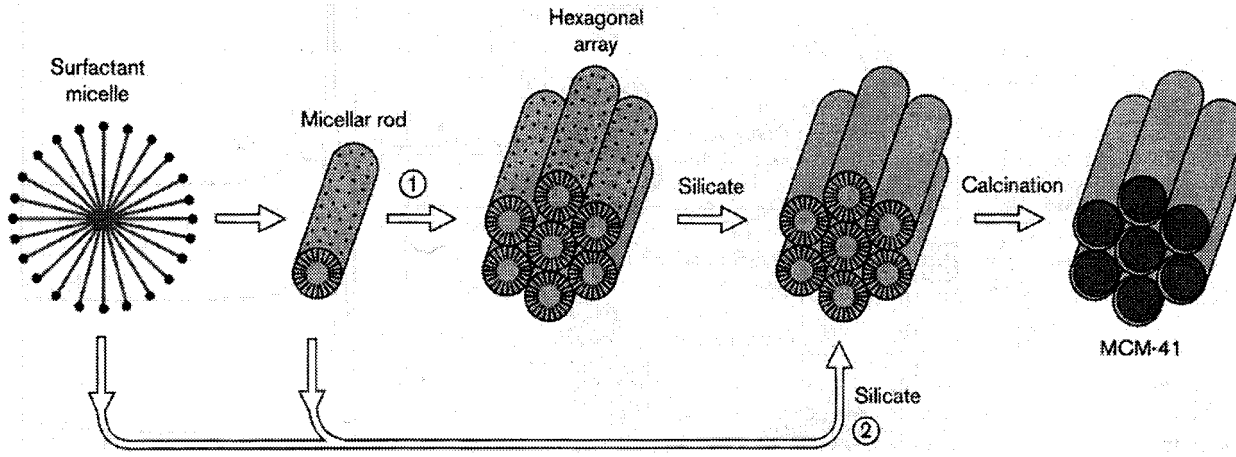

Figure 8. Possible mechanistic pathways for the formation of MCM-41: (1) liquid crystal phase initiated and (2) silicate anion initiated [4].

be present as charge balancing groups associated with the quaternary ammonium surfactant ions. As evidence for this idea, the spacing of the silanol ions was found to be approximately equal to the expected spacing of the quaternary ammonium surfactant ions within the micelles.

Comprehensive accounts describing the synthesis and characterization of MCM-41 using various chain length alkyltrimethylammonium surfactants as templates are readily available in the literature [28, 30, 31]. Characterization has been done by a variety of X-ray and neutron scattering experiments, high resolution and cryogenic transmission electron microscopy (TEM), electron diffraction, scanning electron microscopy (SEM), atomic force microscopy (AFM), sorption measurements, and solid state NMR.

The synthesis and calcination conditions for the alkaline synthesis of MCM-41 were optimized by Edler *et al.* [32], amongst other authors. It was found that calcination should be carried out with care and that the product was most crystalline from unstirred preparations heated at 100°C for no longer than three days. Maximum BET surface areas of 1950 $m^2 g^{-1}$ were attained, with evident crystallinity of the material observed by electron diffraction and TEM. Probably the most ordered MCM-41 material synthesized so far produced X-ray diffraction patterns with up to 7 orders of diffraction in the low angle range, and was synthesized at pH 9–10,

in the presence of sulphate anions [33]. Using such diffraction patterns, a first attempt was made at fitting a form factor to the X-ray (synchrotron) data [34, 35].

The best fit was obtained for a 3-shell pore model (figure 9) consisting of a dense wall region (~0.6 nm thick) and a very low density, spongy ring of silica (~1.3 nm thick), surrounding the void pore (~1.4 nm diameter). Brown *et al.* postulated that in the as-synthesized material, CTAB template molecules occupied what would become the void region after template removal, but also permeated the spongy ring layer of silica. These results contradicted the results obtained from BET adsorption measurements, which suggested a void pore diameter of 38 Å. Density functional calculations have met with some success in extracting pore structure parameters from such isotherm data [36].

More recently, a similar highly crystalline pure silica MCM-41 has been examined using small angle neutron scattering and the contrast variation method [37]. The experiments shed light on various structural features such as template and water distributions, local silica density, and surface properties.

Studies on monitoring the effects of altering surfactant–silica ratios in M41S synthesis gels have led to the isolation of other structures with cubic and lamellar geometries [1, 2, 27, 28]. The lamellar product MCM-50 was found to be unstable to calcination. The cubic M41S material was named MCM-48 and had $Ia3d$ symmetry (by X-ray diffraction, XRD, and by TEM) [38]. An in-depth account of sorption measurements and structure characterization of the cubic material was given in two later papers by Vartuli *et al.* [30, 39].

The precise internal morphology of the $Ia3d$ cubic MCM-48 structure remained unconfirmed for some time. In a more recent paper, the TEM images and XRD patterns obtained for MCM-48 were compared with those generated by a computer simulation of the gyroid minimal surface [40]. The model produced excellent agreement with the experimental characterization, and it was concluded that the gyroid surface was a good description of the MCM-48 mesostructure.

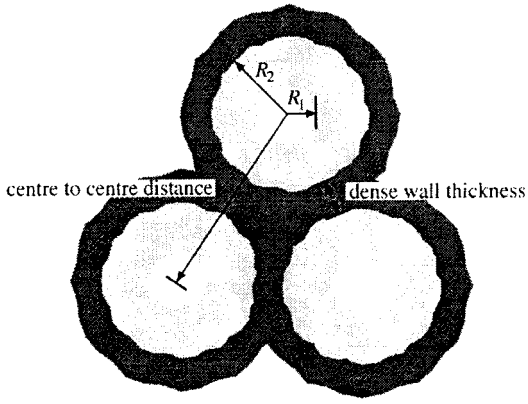

Figure 9. Model of the structure of an MCM-41 pore proposed by Brown *et al.* from their studies using synchrotron X-ray diffraction and SANS [35]. Reprinted with permission from *J. chem. Soc. Faraday Trans.*, 1997, **93**, 199.

MCM-48 was later found to consist of particles with crystal-like faces [41], and single crystals of MCM-48 have been synthesized by Kim *et al.* [42]. The gyroid internal symmetry and the 'cubosome' polyhedral external morphology were combined by Alfredsson *et al.* [41] in an analytical function which could be used to describe the MCM-48 structure. It was speculated that the continuous minimal surface within each cubosome would fold back on itself at the particle periphery to form a closed body. This would seal one of the two interpenetrating channel systems, and leave the other open to the exterior. As each of the two channel systems is chiral, but with opposite handedness, the effect of this would be to produce a chiral open channel structure for each cubosome particle.

Ko and Ryoo [43] described an interesting means of confirming the connectivity of the pores within mesoporous materials, by incorporating platinum wires into the mesopores. The connectivity of the channels is then clearly visible by TEM, and it has been shown that 1-dimensional parallel channels are present in MCM-41, whilst cubic MCM-48 contains 3-dimensional interconnected channels. The method was initially developed to view the channels in a newly synthesized mesoporous product containing a 3-dimensional, disordered network of short, worm like channels of uniform dimension [44].

In the LCT theory proposed by Beck *et al.* [1], silicate condensation was not the dominant rate-determining factor in the M41S structure formation. The structure was defined, instead, by the organization of surfactant molecules into micellar liquid crystals which served as templates for the formation of the silica structure. This suggested that the types of materials which could be formed did not need to be limited to silicates.

Changes in ionic strength, counter-ion polarizability, surfactant concentration, counter-ion charge, temperature, or the addition of co-surfactants or additives (such as alcohols or hydrocarbons) cause liquid crystalline phase changes. Therefore, a change in product structure resulting from the variation of one of the above conditions might be considered as evidence in support of LCT theory (though changes which affect the gel chemistry should also be considered).

5. Mechanistic theories for the formation of M41S silicates

The surfactant concentrations used for the synthesis of M41S materials would be too low, in a purely aqueous

system, for any liquid crystalline structures to be formed. In the M41S synthesis mixtures, silicate ions must therefore play a critical role in triggering the liquid crystal state by serving as counter-ions and stabilizers for the micelle arrays.

Monnier *et al.* [45] presented a detailed model to explain the formation and morphologies of surfactant–silicate mesostructures. They conducted experiments where the formation of the porous silicate was sufficiently slowed down to observe intermediates by X-ray diffraction (see figure 10). For the formation of M41S structures, it was found that initially a short-lived layered material (present for up to the first 20 min of the synthesis procedure) was precipitated, and the hexagonal material appeared later. Three processes were identified:

(1) Multidentate binding of silicate oligomers to the cationic surfactant.
(2) Preferential silicate polymerization in the interface region due to the high concentration of silicate species in this region and the partial screening of their negative charges by the surfactant.
(3) Charge-density matching between the surfactant and the silicate.

A model was proposed which explained the experimental data, including the transformation between lamellar and hexagonal mesophases. The favoured mesophase was taken to be the one which permitted the surfactant head group area, A, to be closest to its optimal value A_o. The overall free energy of the system was taken as:

$$G(A, \rho) = G_{intra}(A) + G_{wall}(\rho) + G_{inter}(A, \rho) + G_{sol}$$

G_{intra} reflects the van der Waals forces and conformational energy of the hydrocarbon chains and of the head groups within a micelle; G_{wall} represents the polysilicate free energy (solvent, counter-ion and silicate van der Waals and electrostatic interactions within the inorganic silicate 'wall'). G_{inter} accounts for the van der Waals and electrostatic effects associated with wall–micelle and micelle–micelle interactions; G_{sol} describes the solution phase energy. ρ specifies the compositions of the various species.

The silicate charge density within the wall, ρ_ε, is compensated by the charges on the surfactant head groups which have an average surface charge density of $1/A$. Therefore the electrostatic interactions link A_o with ρ_ε. The relation between the two is called 'charge density matching'. In surfactant–silicate systems, polymerization driven by G_{wall} affects ρ_ε, providing a mechanism to explain the transition between lamellar and hexagonal mesophases.

In the early stages of synthesis, the presence of highly charged silica oligomers favours a small value of A_o (i.e. a more concentrated surfactant surface charge). As polymerization of the silicate progresses, the anionic silanol group density diminishes so A_o increases (concentration of compensating cations decreases). The silicate wall is still poorly condensed during the early stages of the synthesis, allowing the system to increase A towards A_o by adopting the hexagonal structure (figure 11) according to charge-density matching criteria. The resulting structure had clearly hexagonal as opposed to circular pore shape, probably due to the fact that silicate species only accumulated at the surfactant interface to the extent necessary for charge compensation. The walls must therefore have been of uniform thickness.

Monnier *et al.* made the following predictions based on their observations:

(1) The lamellar phase would be favoured at high pH and for a low degree of polymerization of the silicate source.

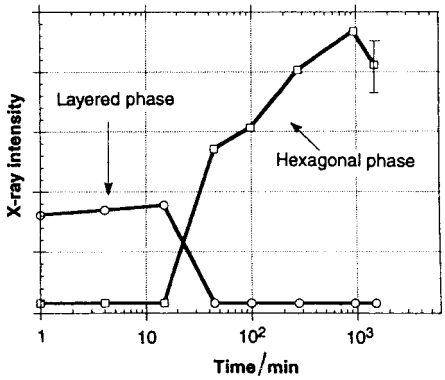

Figure 10. Time evolution of the intensity of X-ray diffraction features associated with layered and hexagonal (M41S) mesostructures at 348 K [45].

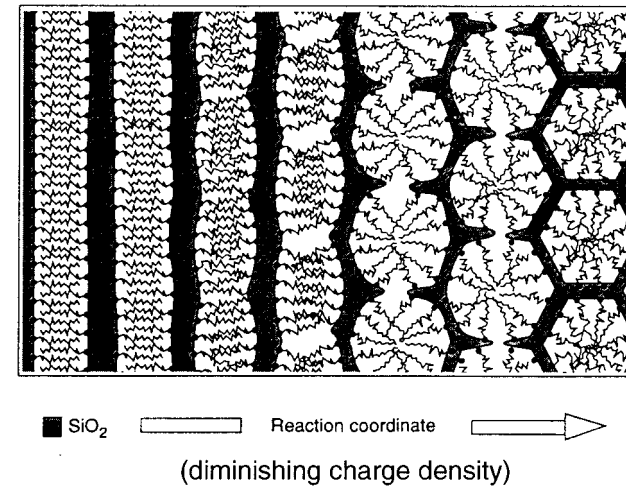

Figure 11. Schematic of the mechanism proposed for the transformation of a surfactant–silicate system from the lamellar to the hexagonal mesophase [45].

(2) At low pH and for highly polymerized silica the hexagonal phase would be favoured.

The effects of pH on a synthesis gel containing sodium silicate and cetyltrimethylammonium chloride (CTACl) were recently investigated by Luan *et al.*, [46] and the results generally supported the predictions made by Monnier *et al.* The bicontinuous cubic phase, MCM-48, would form when the value of A_o (set by the reaction conditions) is close to the head group area required for the $Ia3d$ phase. G_{intra} and G_{inter} play a leading role in determining the final product geometry. Charge-density matching establishes a link between the chemical composition and structure of the silicate wall and the formation of a particular mesostructure.

Alfredsson *et al.* [47] conducted experiments where the synthetic reaction of MCM-41 was followed by TEM. The transition from lamellar to hexagonal symmetry was observed during the synthesis. Steel *et al.* [48] made a study by ^{14}N NMR of cetyltrimethylammonium chloride surfactant mesophases during the synthesis of M41S mesoporous silicates. Again, both lamellar and hexagonal phases were observed, depending on the initial silicate concentration. The mechanism suggested (figure 12) involved the silicate oligomers initially dissolving into the aqueous regions around surfactant micelles and condensing into layers. The confined micelles then formed hexagonal surfactant mesophases. At low silicate concentrations, puckering of the silica layers would lead to hexagonal phases, whilst at higher silicate concentrations, the thicker layers would resist puckering and remain as the lamellar phase. Further information on the silica condensation mechanism was obtained by ^{29}Si NMR from which an accurate ratio of incompletely condensed silicon atoms (Q^3) to completely condensed silicon atoms (Q^4) was calculated [49].

Chen *et al.* [50] confirmed from an *in situ* ^{14}N NMR study of the M41S system that no liquid crystal phase was present in the reaction medium throughout the synthesis of MCM-41. It was suggested, however, that rod-like surfactant micelles formed through the hydrophobic effect at these concentrations of surfactant and other ions. The silicate species interacted with the surface of these micelles, either by coulombic interactions (for ionic surfactants) or hydrogen bonding (for neutral surfactants), to form silica-coated micellar precursors. These would then condense into the final structures under hydrothermal conditions. This mechanism contradicted the theories that suggested the formation of layered intermediates. However, it should be noted that the formation mechanisms will depend heavily on the synthesis routes chosen: different silica sources, pH, and/or surfactant template concentrations will lead to particular formation mechanisms. The mechanism of Chen *et al.* is depicted by route A1 in figure 13.

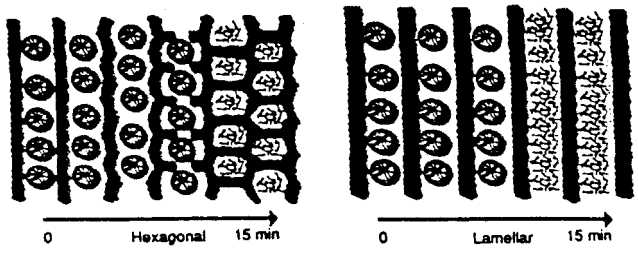

Figure 12. Formation of hexagonal and lamellar M41S [48]. Reprinted with permission from *J. chem. Soc., Chem. Commun.*, 1994, 1571.

Stucky and co-workers [8, 29, 45, 51–55] postulated that due to the dynamic nature of the interaction between inorganic and organic species throughout the synthesis, different products would result from a minor change in the M41S synthesis conditions. This theory was supported by an *in situ* small angle neutron scattering (SANS) study, with the scattering contrast adjusted to enhance/diminish scattering associated with the organic or the inorganic phases of the synthesis mixture [56]. SANS was used to probe intermediate structures as they changed throughout the reaction. It was observed that no pre-assembled micellar arrays existed in the bulk synthesis gel, confirming the ^{14}N NMR results obtained by Chen *et al.* and Steel *et al.* [48, 50]. Calabro *et al.* conducted an *in situ* ATR/FTIR study on M41S-type synthesis gels which led to similar conclusions [57].

Cheng and co-workers found that MCM-41 could be synthesized at surfactant concentrations as low as, but not lower than the critical micelle concentration (CMC) [58]. This observation can be taken as proof for the micellar templating mechanism. Absence of surfactant invariably yielded an amorphous material. The rate of silicate polymerization was also found to increase by a factor of more than 2000 when surfactant was present in the synthesis mixture. The rate increase was taken as evidence for the electrostatic interactions between surfactant and inorganic species, which bring the silica oligomers close together and favour the polymerization reaction. The morphology of MCM-41 particles was observed by TEM, and it was seen that the individual crystallite edges met at an angle of 120°. It was proposed that the morphology of the MCM-41 particles was proof of a silicate anion-initiated mechanism for growth, rather than a mechanism involving a layered intermediate [59].

Huo *et al.* [29, 60] suggested a generalized charge density matching mechanism whereby mesostructures precipitate out of solution at concentrations well below those required for liquid crystal formation. Route A2 in figure 13 depicts how inorganic tubular mesostuctures (products of route A1) are formed via a charge density

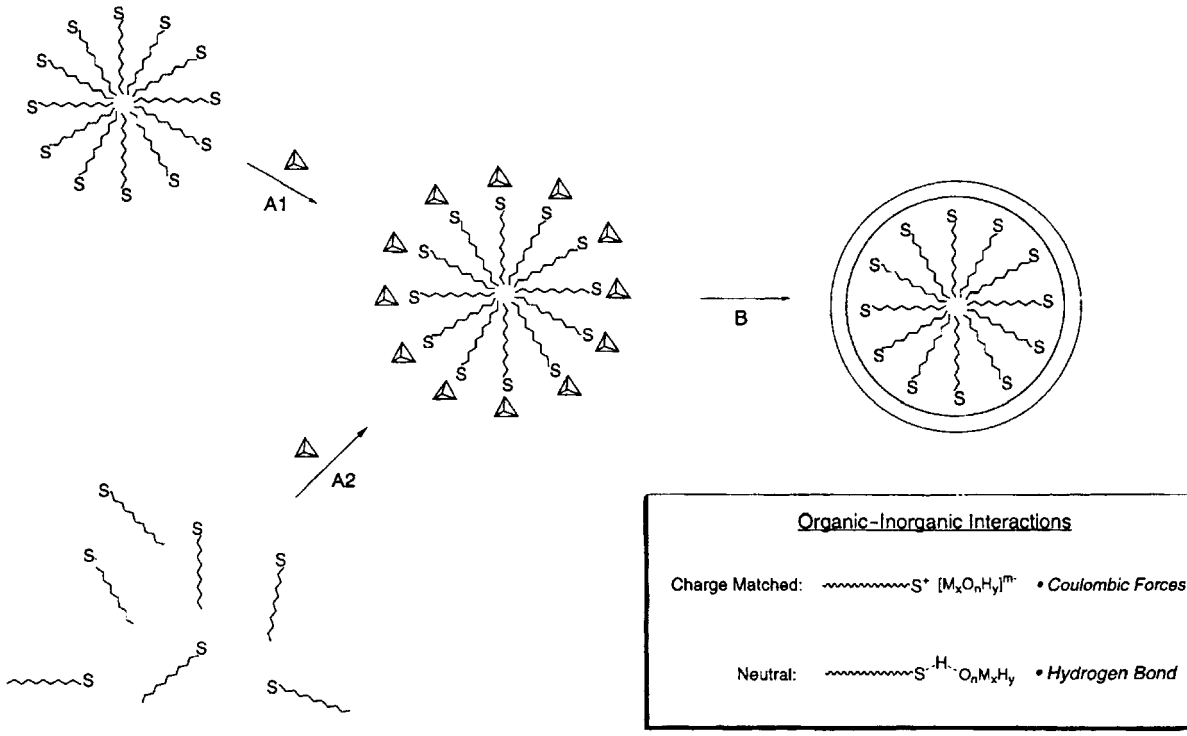

Figure 13. Generalized scheme for the formation of inorganic tubular mesostructures using charged or neutral surfactants [5]. Route A1 depicts the mechanism proposed by Chen *et al.* [50]; route A2 depicts the charge density matching mechanism described by Huo *et al.* [29, 60]. S denotes the surfactant head group; x, y and n denote the stoichiometries in the cluster of the metal (M), hydrogen, and oxygen, respectively. m denotes the charge on the entire cluster; the charge depends on the number of oxygen and hydrogen atoms in the cluster, as well as the nature of M. Tetrahedra represent inorganic precursor units.

matching mechanism, without the formation of intermediate rod-shaped micelles. The balancing of charge density and size of the surfactant head groups is considered an important factor in determining the type of mesostructure formed on precipitation.

Regev has described a study of the intermediate structures formed during MCM-41 hydrothermal synthesis [61]. It was found that the synthesis began with an initial induction phase, followed by nucleation of numerous M41S nuclei. The structured product was identifiable by small angle X-ray scattering (SAXS) after a few hours. The regular structure of the M41S material became better defined as the crystallization time was lengthened. It was concluded that clusters of elongated micelles were responsible for the structure in the final product. These were in turn formed from a spherical to elongated micelle transition resulting from the addition of the silica source to the surfactant–base–water system.

Firouzi *et al.* identified multiply charged, double-four ring (D4R) silicate oligomers in the alkaline MCM-41 synthesis mixture [54]. It was suggested that these have a multidentate interaction with the cationic surfactant head group, which is favoured over the coulombic attraction between surfactant and bromide ions. In a more recent publication by the same authors, a comprehensive study of the chemical and structural characteristics of alkaline lyotropic hexagonal and lamellar silicate–surfactant liquid crystal phases was presented [62]. This was the first study providing such detailed insight into the molecular processes governing mesophase formation in M41S-type systems. Additives, namely tetramethylammonium hydroxide (TMAOH) and methanol, were added to the silicate–surfactant gels to stabilize the highly charged, D4R silicate oligomers, $[Si_8O_{20}H_n]^{(8-n)-}$. This effectively meant that the silicate–surfactant self-assembly process was decoupled from silicate polymerization effects. The theory behind phase separation of ordered mesophases from highly alkaline isotropic aqueous surfactant precursor solutions was discussed in detail. Repulsive interaggregate interactions predominate over van der Waals attractive forces in single phase CTAB isotropic micellar solutions. It was suggested that addition of highly alkaline silicate electrolyte induces an overall shift in force balance, favouring attractive van der Waals interaggregate interactions, causing a surfactant-rich phase to separate from the water-rich isotropic phase. In the phase-separated system, the two phases are in thermodynamic equilibrium [62].

The phase separation was explained in terms of a combination of reduced Debye length (the characteristic

diffuse double layer thickness) associated with inter-aggregate repulsion, and an increased relative importance of the van der Waals attractive force between surfactant aggregates. The Debye length is inversely proportional to the charge of the electrolyte solute molecules in micellar systems [63]. For these systems, the additivity of molecular van der Waals (vdW) forces leads to long range vdW interaggregate interaction forces which scale as d^{-1} or d^{-2} (d is the interaggregate separation). This is a major increase with respect to the short range ($\propto r^{-6}$) vdW effects for single molecules [63]. The presence of micelles in the surfactant precursor solution, which promotes these long range vdW interactions, is therefore an important prerequisite for mesophase formation in these systems. This last theory is substantially supported by experiment.

In their experiments Firouzi *et al.* used ^{2}H NMR, small angle XRD and polarizing microscopy to gain information on aggregate geometry and symmetry of the mesophase, and to quantify the silicate–surfactant liquid crystal cell parameters [62]. ^{13}C NMR provided further information on the mobility of the surfactant chains, showing that the cetyltrimethylammonium cations had liquid-like mobility within the micelles. ^{2}H, ^{29}Si and ^{81}Br NMR measurements on the aqueous solutes of the liquid crystal provided further information on the complex aqueous silicate chemistry of the system. Silicate–surfactant liquid crystal phase transformations were induced by manipulating the system variables (temperature and composition). In the absence of silicate polymerization, the lamellar to hexagonal phase transformation was found to be completely reversible [62].

An *in situ* X-ray diffraction study of the kinetics of MCM-41 synthesis showed the formation of a hexagonal mesophase within the first 3 minutes of reaction [64]. There was no sign of an intermediate phase. The study was carried out using a purpose-made reactor connected to a cell specially designed for X-ray diffraction measurements on liquids. The silica precursor used was TEOS, which has a low solubility in water. It was therefore suggested that the formation mechanism for this system originated from an initial oil-in-water emulsion. Further information was recently provided about the kinetics and mechanism of micelle-templated silica formation from a computer-aided analysis of electron paramagnetic resonance (EPR) spectra of probes inserted in the micelles [65]. The synthesis was found to consist of two steps. In the first, silicate species coated the micelles and 'froze' them; in the second step there was an increased interaction between the surfactant cationic head groups and the solid walls of the silica, resulting in the characteristic hexagonal mesophase.

5.1. *Charge density matching*

In the generalized approach to the synthesis of mesoporous inorganic materials described by Huo *et al.* [29], charge density matching is the main factor controlling the products formed. By combining the appropriately charge-balanced surfactant and inorganic species, a plethora of mesophase materials could theoretically be formed. The charge balancing approach implied that either cationic or anionic surfactants could be used to synthesize cationic or anionic frameworks. To a significant extent, the charge density matching theory has been supported by experiment. Figure 14 summarizes the four possible charge density matching routes, and provides examples of materials formed via each route.

In a more recent paper, Huo *et al.* [66] described the synthesis of several silica-based materials. Covalent organosilanes, quaternary ammonium surfactants and mixed surfactants in various reaction conditions were used to synthesize MCM-41 (2-D hexagonal, $p6mm$), MCM-48 (cubic $Ia3d$), MCM-50 (lamellar), SBA-1 (cubic $Pm3n$), SBA-2 (3-D hexagonal, $P6_3/mmc$), and SBA-3 (2-D hexagonal, $p6mm$) from acidic synthesis media. Mixed CPCl (cetylpyridinium chloride)/CTACl surfactant systems have been used to template MCM-41 type materials [67]. As the CPCl:CTACl ratio was decreased, a gradual increase in the d_{100} spacing of the mesoporous material was observed. Therefore, varying the ratio of mixed surfactants leads to fine-tuning of pore dimensions. From existing experimental data, surfactants and synthesis conditions can now be chosen and controlled to obtain predicted silica-based mesophase products.

6. Developments on the dilute regime synthesis

Since the discovery of M41S materials by Mobil scientists in 1992, a great deal of work has been directed towards refining the dilute regime synthetic procedure, and improving the properties of the resulting mesoporous materials. Mesoporous materials are metastable forms of metal oxides (e.g. siliceous MCM-41 is thermodynamically a great deal less stable than quartz) and are generally synthesized at low temperatures (25 to 100°C) so that the condensation reactions are kinetically controlled [68].

One main characteristic of all M41S materials is that on an atomic scale the silica mesopore walls are amorphous, which means that these materials are thermodynamically metastable. The metastability of the MCM-41 silica walls was highlighted by work conducted by Kloetstra *et al.* [69, 70] who, on recrystallizing MCM-41 and MCM-48, produced mesoporous materials containing small amounts of framework ZSM-5, or other higher stability silicate species.

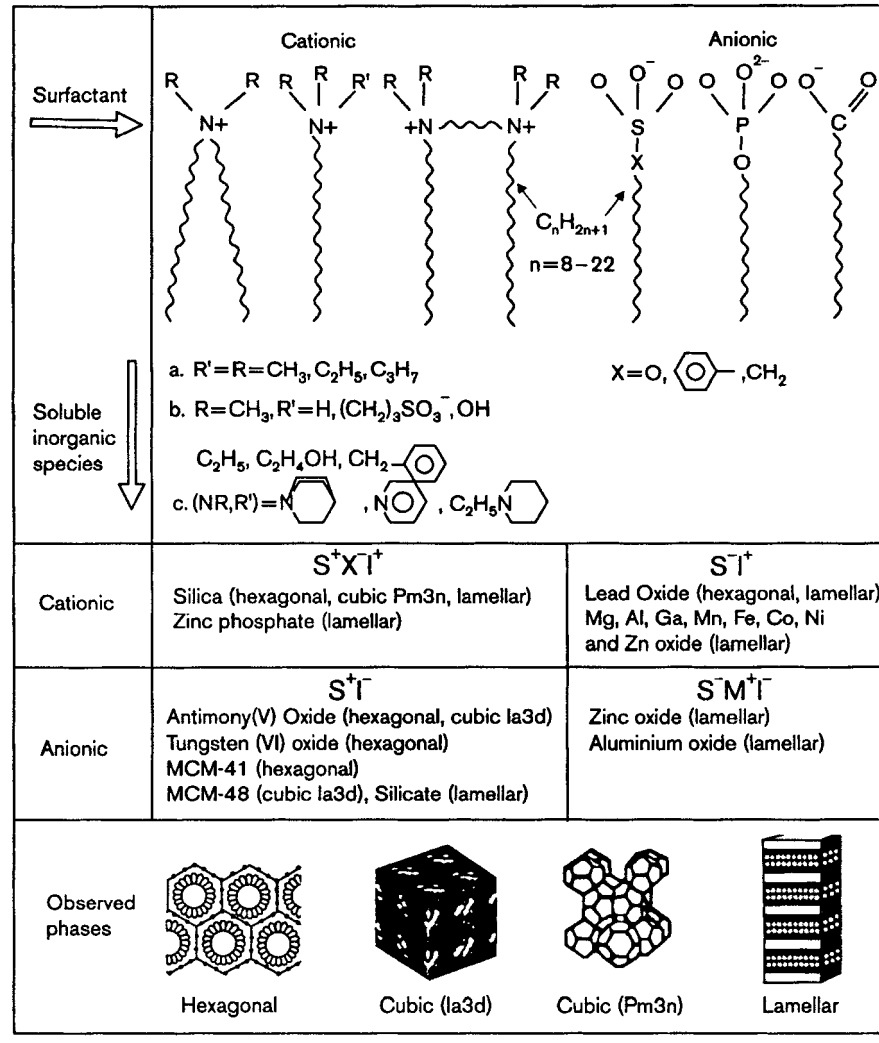

Figure 14. Synthesis pathways using different combinations of surfactant and soluble inorganic species. S is the surfactant, X is a halide ion, M is a metal ion and I is the inorganic ionic precursor [29].

It was found that due to silicate hydrolysis, mesoporous MCM-41 and MCM-48 tended to disintegrate when kept in water at 370 K [71]. To a great extent the problem of low hydrothermal stability of the M41S materials in boiling water was overcome by using various salts such as sodium chloride, potassium chloride, sodium acetate, and ethylenediaminetetra-acetic acid tetrasodium salt during the hydrothermal crystallization process. Very high stability MCM-41 products were obtained, which showed negligible structure degradation during heating for 12 h in boiling water [72]. Kim *et al.* also reported [71] that post-synthetic ion-exchange of aluminosilicate AlMCM-41 with Na^+, K^+, Ca^{2+} and Y^{3+} led to materials with higher hydrothermal stabilities. The hydrothermal stability trend for the ion-exchanged materials was: Y^{3+} (stable to 1170 K)$\approx Ca^{2+} > Na^+$ (stable to 1070 K)$\approx$ as-calcined AlMCM-41 > pure silica MCM-41 (stable to 980 K).

M41S materials have been synthesized in both basic and acidic media [60], and all the variables (such as pH, gel composition and temperature) in the process have been thoroughly investigated by various research groups. Complete phase diagrams for the M41S synthesis gels, such as the one illustrated in figure 15 are now available in the literature [73].

A fundamental difference between acid-catalysed and base-catalysed M41S synthesis is that in the as-synthesized products, the silica walls have neutral charge in the acid preparations, whilst in the basic preparations negatively charged silica walls are formed. In the former material, the cationic surfactant is charge-balanced by a single halide ion, and can be easily removed by a water/ethanol solvent wash. For the alkaline synthesis product, the surfactant template needs to be removed by acid washing (ion exchange) or by calcination.

Much work has been directed at decreasing synthesis temperatures and time, as well as controlling pore dimensions and crystallite size. Control of the rate of silicate polymerization by adjusting the pH initially led to badly

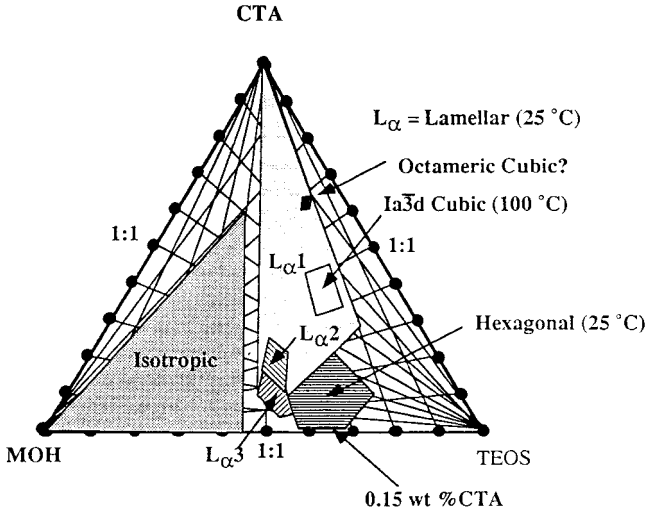

Figure 15. Synthesis phase diagram of silicate mesostructures [51, 73]. Reactions were carried out at room temperature except for the cubic phases which were synthesized at 100°C. A large excess of water component was also present in all of the mixtures. MOH = methanol; CTA = cetyltrimethylammonium surfactant ($C_{16}H_{33}N(CH_3)_3^+ Br^-$); TEOS = tetraethoxysilane.

condensed silica walls and hydrothermally unstable products in alkaline media [51]. Later work using different pH conditions, controlling the aluminosilicate reactivity in the synthesis gels, produced materials with thicker pore walls and improved thermal and hydrothermal stabilities [72, 74–78]. A room temperature synthesis method was described which led to equally stable mesoporous products to those produced at higher temperatures [79].

The effect of gel ageing time, temperature, stirring, source of silica and alkyltrimethylammonium template (CTAB or CTACl), and overall concentration of the reactants on the quality of the MCM-41 product was studied by Cheng *et al.* [80] It was found that highly basic gels, or gels containing low silicate concentrations favoured lamellar products. The most highly crystalline MCM-41, with the most orders of diffraction in the powder X-ray diffraction pattern, was obtained from a gel with molar composition SiO_2 : 0.19 TMAOH : 0.27 CTAB : 40 H_2O, aged at 20°C for 24 h followed by reaction at 150°C for 48 h.

In the original papers describing the synthesis of M41S materials [1, 2], the pore diameters of the mesoporous materials were determined by the choice of surfactant template, and also by the use of an auxiliary organic molecule, mesitylene (1,3,5-trimethylbenzene). Pore diameters ranging between 15 and 100 Å were obtained. More recently *n*-alkanes of different chain lengths were used as swelling agents for the mesoporous products [81]. The pore diameters of the products increased proportionally with the length of the *n*-alkanes, containing up to 15 carbon atoms.

The pore diameter of mesoporous products has also been controlled by adjusting the synthesis gel and crystallization variables. In the presence of tetramethylammonium cations, mesoporous products were formed after 24 h, and the pore size increased for longer crystallization times (see figure 16) [82]. Similar results were obtained by Cheng *et al.*, who varied the pure silica MCM-41 channel diameter between 26.1 and 36.5 Å and found that the wall thickness varied between 13.4 and 26.8 Å, simply by using different synthesis temperatures (70 to 200°C) and/or reaction times [83]. MCM-41 with wider pores, thicker walled channels and higher degrees of polymerization were obtained for longer reaction times. The MCM-41 structure with the thickest walls (26.8 Å) could withstand temperatures as high as 1000°C without disintegrating.

The suggested explanation for the pore expansion with increasing reaction time was as follows: as reaction times are increased, the pore size of the MCM-41 product increases, reaching an upper limit very close to the diameter of a CTAB micelle. At high temperatures (165°C in the work of Cheng *et al.*), some surfactant cations decompose to neutral $C_{16}H_{33}(CH_3)_2N$ molecules, which locate themselves in the hydrocarbon core of the micelle. This has the effect of increasing the micelle diameter, and therefore the MCM-41 pore size. There is, however, an upper limit to the number of neutral amine molecules that the micelles can accommodate in their core, leading to an upper limit in the swelling effect [83].

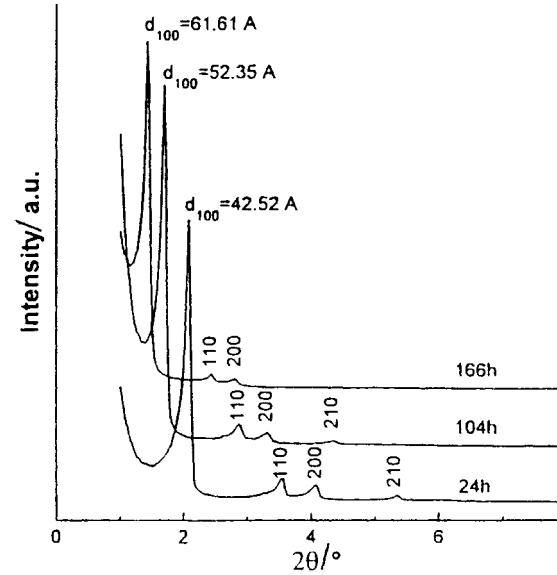

Figure 16. XRD (CuK_α) of MCM-41 samples with different pore diameters after 24, 104, and 166 h reaction times [82]. Reprinted with permission from *Chemical Reviews*, 1997, **97**, 2373. Copyright 1999 American Chemical Society.

Further work was carried out by Sayari *et al.* who used hydrothermal restructuring of MCM-41 to produce large pore MCM-41 products [84]. It was shown that the pore size enlargement was accompanied by a significant improvement of pore size uniformity, a gradual decrease of the specific surface area, and pore wall thickening. Additionally, hydrothermal post-synthetic treatment of MCM-41 led to the formation of considerable amounts of micropores in addition to their characteristic mesopores (*c.* 3 nm). The relative amount of micropores and mesopores was shown to be dependent on the treatment conditions. It was suggested that post-synthetic hydrothermal restructuring is a convenient synthesis route for MCM-41 silicates with a bimodal pore size distribution with controllable amounts of microporosity [85].

The crystallite size is of particular importance for mesoporous materials containing unidirectional channels, as in MCM-41. If the mesopores are long, which might be the case in large crystallites, diffusion problems could occur. In these cases it is preferable to have a very small crystallite size. Small particles of MCM-41 are obtained if reaction times are kept short, i.e. the mesoporous product nucleates, but has little time to grow into larger particles. Cutting the reaction times can, however, jeopardize the silica condensation process leading to poorly polymerized products. Microwave heating overcomes this problem by speeding up the condensation step, allowing high quality products to form in times as short as 1 h at 150°C [86–89]. The resulting MCM-41 crystallites are very small (approximately 100 nm diameter).

Aluminosilicate MCM-41 has been studied a great deal, in parallel with the pure silica analogues. Aluminium was introduced into the MCM-41 structures either by including an Al source in the synthesis gels or by treating the pure silica MCM-41 post-synthetically [90–97]. Hamdan *et al.* aluminated purely siliceous mesoporous [Si]-MCM-41 using an aqueous solution of sodium aluminate, $NaAlO_2$, to form [Si,Al]-MCM-41 with the framework Si/Al ratio as low as 1.9. They found, however, that upon treatment with a concentrated ($> 1\ mol\ l^{-1}$) solution of $NaAlO_2$ at moderate temperatures (100 ± 20°C), [Si]-MCM-41 was transformed into crystalline zeolite Na-A [98].

The synthesis parameters for the synthesis of both pure silica and aluminosilica MCM-48 were optimized by Romero *et al.* [99, 100]. For the pure silica MCM-48 synthesis, the effects of changing the silica concentration, surfactant template (CTAB or CTACl), and the reaction time were studied by continuous sampling and analysis. Increased synthesis times produced mesophases in the following trend: hexagonal phase–cubic phase–lamellar phase. The cubic phase was preferentially formed when the hydroxide concentration and the surfactant/silica ratios were high in the synthesis mixture. CTAB produced better structured materials than CTACl [99]. AlMCM-48 was synthesized using aluminium chloride hexahydrate and aluminium sulphate as aluminium sources in the synthesis gels. Si/Al atomic ratios of 15 to 40 in the AlMCM-48 products were obtained, but the structure quality of the product deteriorated as the Al content was increased [100].

Large head group cationic surfactants such as $C_{16}H_{33}N(C_2H_5)_3Br$ with acid or base synthesis conditions lead to 3-dimensionally structured silica products containing cage-like voids, with dimensions somewhat larger than the channel diameters measured for the M41S materials. SBA-1 is a cubic cage mesostructure with $Pm3n$ space group symmetry, and SBA-2 is a 3-dimensional hexagonal cage structure with $P6_3/mmc$ symmetry [29, 66].

6.1. *Neutral templating routes*

A dilute regime method for the synthesis of mesoporous solids was reported where the template was a non-ionic surfactant (a primary amine or polyethylene oxide) and the silica precursors were non-ionic silicon esters such as TEOS [101, 102]. The template was thought to interact with the silica precursor by hydrogen bonding. The mesoporous products resembled M41S materials, but had slightly less long range order. They were reported to have thicker silicate walls, smaller crystallite size, and improved textural mesoporosity (improved access to framework pores). Materials templated via this neutral route also had superior thermal stability upon calcination in air with respect to MCM-41 materials [103]. The neutral synthesis system had the added advantage that the surfactant could be removed by neutral solvent extraction, avoiding the calcination step which often damaged the mesoporous structure. Further improvements on the synthesis procedure were reported in a later paper [104].

A neutral alkoxide/polyoxyethylene surfactant templating route was also used to produce mesoporous products with the pores arranged in random worm-like motifs, with no distinguishable hexagonal or cubic long range ordering [105]. The products, named MSU-X, were formed by firstly obtaining a homogeneous alkoxide/surfactant solution by ageing at room temperature, and secondly initiating the mesophase assembly by adding fluoride ions. Fluoride ions had previously been shown to catalyse alkoxide hydrolysis and mesostructure cross linking [106]. The pore size of the mesoporous product could be increased by increasing the synthesis temperature, and was varied by as much as 2.4 nm. The MSU-X pore-size distributions were sharp, but the products were not as highly ordered as the M41S materials. BET surface areas were also somewhat lower than for the M41S

structures, and were measured to be between 570 and 850 $m^2 g^{-1}$.

6.2. *Gemini surfactants as templates*

Templating experiments were conducted where dual chain dialkyldimethylammonium salts (gemini surfactants) were used as the templating agents [107, 108]. The gemini surfactants had the generalized molecular formula $C_{16}H_{33}(CH_3)_2[(CH_2)_nCH_3]N^+$, where $n = 1–12$, and can be represented as shown in figure 17. For odd n (1, 3, 5, 7), hexagonal MCM-41 was produced. For even n (2, 4, 6, 8) and any n greater than 7, the product was a lamellar phase. When n was greater than 7, the surfactant appeared to behave as a two-tailed molecule which favoured bilayer formation. No explanation has yet been provided for the observed alternation of products when n was smaller than 7.

Huo *et al.* [55, 109] used somewhat different gemini surfactants (see figure 18) as templates for a whole range of mesoporous structures: MCM-41 (2D hexagonal, $p6mm$); MCM-48 (cubic, $Ia3d$); MCM-50 (lamellar); SBA-1 (cubic, $Pm3n$), SBA-2 (3D hexagonal, $P6_3/mmc$) and SBA-3 (2D hexagonal, $p6mm$). A new mesoporous supercage structure, SBA-2, which was analogous to a zeolite cage structure was also synthesized. The cages could be dimensionally tailored by changing the surfactant, but no known liquid crystal counterpart existed for the cage structure.

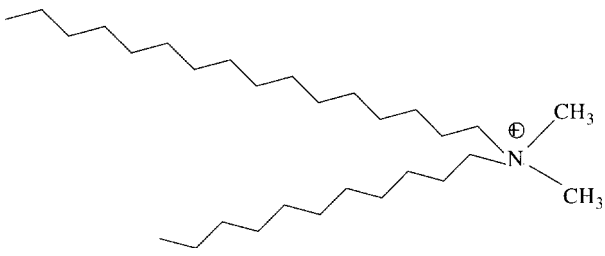

Figure 17. Schematic representation of a gemini surfactant, as used by Karra, Sayari and co-workers [107, 108].

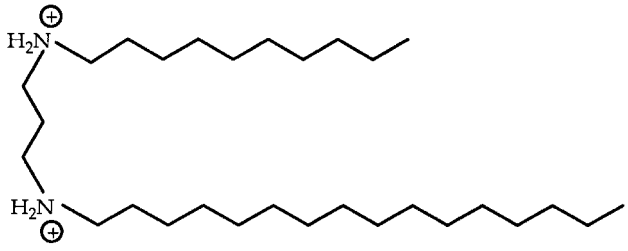

Figure 18. Schematic representation of the gemini surfactants used by Huo *et al.* [55]. The two quaternary ammonium head groups are linked together by a short alkyl chain, and an additional long hydrocarbon chain is attached to each head group.

6.3. *Large pore silica via colloidal crystallization*

Silica containing a 3D ordered array of pores of uniform dimension has been synthesized by mineralizing the cavities between arrays of colloidal-sized latex spheres (200 to 1000 nm) in a colloidal crystal [110]. The colloidal particle surfaces were functionalized by adsorption of CTAB, to induce silica polymerization. The pore sizes of the calcined materials ranged, controllably, from approximately 150 nm to 1 μm.

Pellets of inorganic oxide containing highly monodisperse macropores (50 nm to several μm in diameter) have been synthesized from an emulsion containing equally sized organic droplets which self-aggregated into a nearly crystalline array [111]. After drying and heat treatment, the inorganic materials contained spherical pores, where the emulsion droplets were previously located. Macroporous titania, silica and zirconia materials were produced in this way, and the authors claim that templating of non-aqueous emulsions is a versatile means of producing ordered macroporous ceramics of many different materials.

6.4. *Polymer templates*

Ultra large pore hexagonal and cubic mesoporous products have recently been synthesized using non-ionic poly(alkylene oxide) triblock copolymers as structure directing agents and tetra-alkoxysilane silica sources, in acidic media (pH < 1) [13, 112]. The hexagonal SBA-15 product was synthesized with a wide range of uniform pore sizes and pore wall thicknesses at low temperatures (35 to 80°C), using a variety of poly(alkylene oxide) triblock copolymers and by the addition of cosolvent organic molecules. One example of a tri-block copolymer used was poly(ethyleneoxide)-poly(propyleneoxide)-poly-(ethyleneoxide), PEO-PPO-PEO. The method was found to be very versatile: structured products were obtained using tetramethoxy-, tetraethoxy- and tetrapropoxy-silanes (TMOS, TEOS and TPOS) as silica sources, and a whole range of acids was used to obtain the required synthesis gel pH (HCl, HBr, HI, HNO_3, H_2SO_4 or H_3PO_4).

The as-synthesized SBA-15 material was a 2-dimensional hexagonal (space group $p6mm$) silica-block copolymer mesophase. Calcination at 500°C produced highly ordered materials with uniform pore diameters of 46 to 300 Å, silica wall thicknesses between 31 and 64 Å and pore volume fractions of up to 0.85. The block copolymer template could also be removed by solvent extraction with ethanol and by heating at 140°C for 3 h, for recycling. The mesoporous product was hydrothermally stable in boiling water [112]. The cubic mesoporous cage structure had space group symmetry $Im3m$, and was synthesized using PEO-PPO-PEO block copolymer templates with relatively high EO/PO ratios [13]. These

materials had pore sizes > 80 Å, and were also found to be hydrothermally stable. A further cubic $Pm3m$ phase was obtained with oligomeric non-ionic surfactants.

A block co-polymer/non-aqueous solvent structured phase has been used to template organically modified aluminosilicate lamellar and hexagonal mesostructures [113]. The block copolymer template was poly(isoprene-b-ethylene oxide); (3-glycidyloxypropyl)trimethoxysilane and aluminium *s*-butoxide were the silica and aluminium sources, respectively. The composite materials formed were highly ordered on a length-scale of 40 nm. The morphology of the porous products was varied by using different initial amounts of metal alkoxide in the synthesis gels. The pore size and state of alignment of the synthesized materials were also controlled. The stability of the structure to calcination was not reported.

Both the above studies showed that the dimensional range of ordering offered by mesoscopic liquid crystal phases in classic LCT synthesis can be greatly extended by using block copolymer phases as the structure-directing media for inorganic oxide mineralization. Pore sizes on polymer-templated products are about an order of magnitude larger than M41S pore sizes.

7. Mesoporous silica derived by intercalation of layered polysilicate kanemite

Virtually at the same time as M41S mesoporous silicas were first being synthesized, Inagaki *et al.* [114–117] reported the synthesis of hexagonally packed channels from layered polysilicate kanemite. The mesoporous product was named FSM-16. The mechanism for the formation of this material is very different from the silicate anion-initiated MCM-41 synthesis and has been shown to occur via intercalation of the kanemite layers with surfactant molecules, see figure 19.

Kanemite consists of flexible, poorly polymerized silicate layers which buckle around the intercalated surfactant molecules. Vartuli *et al.* [118] compared M41S materials resulting from LCT with the products resulting from intercalation of layered polysilicates. Both methods used alkyltrimethylammonium surfactants as templates, but the mechanisms of formation, silicate anion initiated LCT and intercalation, were very distinct. The MCM-41 resulting from the LCT mechanism was found to have five times the internal pore volume of the layered silicate-derived material, and the pore size distribution was found to be sharper than for FSM-16. Figure 20 depicts the formation of three different types of mesoporous material and their powder diffraction patterns.

The kanemite-derived materials were more highly condensed and exhibited thicker silicate walls than the M41S materials. Chen *et al.* suggested that the thermal and hydrothermal stability of FSM-16 was somewhat better than for MCM-41 [119]. A full characterization of the kanemite-derived mesoporous silica product was described in a later reference by Inagaki *et al.* [120]. From water adsorption measurements, a type 5 isotherm was obtained which suggested that the internal silica surface was hydrophobic [121]. Nitrogen physisorption on the kanemite-derived mesoporous solid has been reported by Branton *et al.* [122]. Aluminium-containing materials have been formed recently using this synthesis method, by treating the original layered silicate with an aluminium source before intercalation with the surfactant, to form the hexagonal mesoporous product [123].

8. True liquid crystal templating (TLCT) of mesoporous materials

Attard *et al.* successfully synthesized mesoporous silica from synthesis gels containing non-ionic polyoxyethylene (POE) surfactants at concentrations required to form liquid crystal phases at room temperature [124]. The syntheses were carried out at room temperature, under mildly acidic conditions (pH 2). TMOS was the silica precursor, which hydrolysed in the aqueous regions of the liquid crystal phases and then polymerized to solid silica. At pH 2, the silicate polymerization kinetics were slow, and were therefore decoupled from the self-assembly of the surfactant micelles. The methanol produced during the hydrolysis of the TMOS was removed throughout the synthesis procedure by keeping the synthesis gel under constant vacuum. Hexagonal, cubic and lamellar products were obtained, and the former two were stable to calcination.

For the synthesis of the hexagonal mesoporous product, the synthesis gel consisted of a 1 $C_{12}EO_8$(†): 1 (10^{-2}M) HCl: 2.11 TMOS weight ratio of reactants. The gel was placed under vacuum overnight, at room temperature, to produce the mesoporous as-synthesized product. Striking similarities were observed by polarizing

†Octaethylene glycol monododecyl ether.

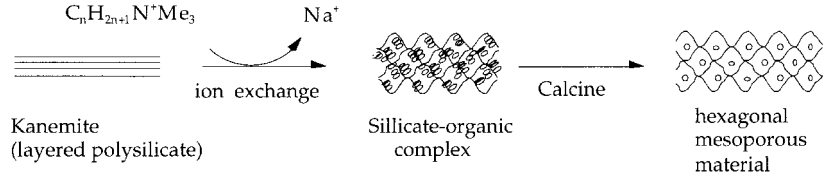

Figure 19. Scheme showing the mechanism of formation of hexagonal mesoporous FSM-16 from kanemite.

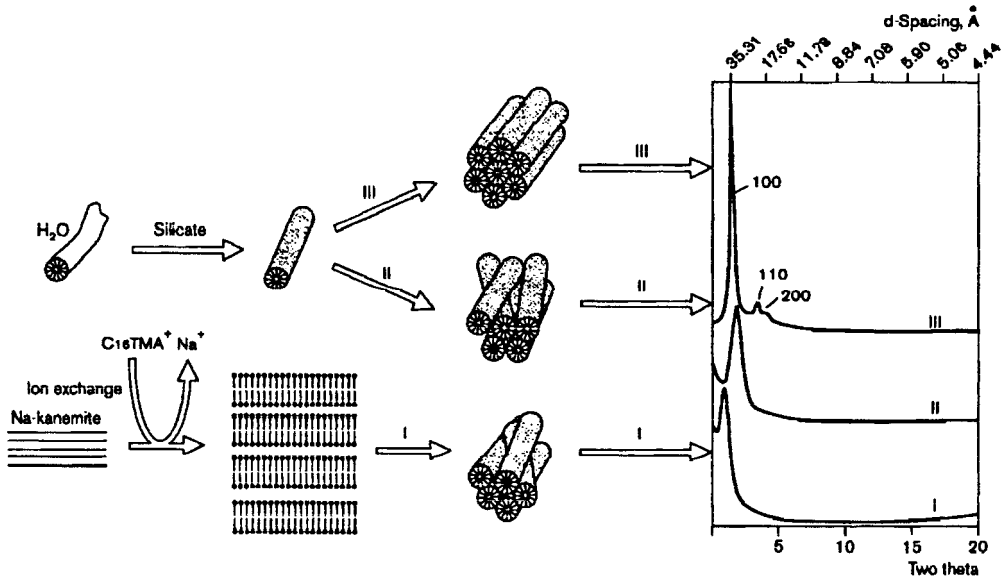

Figure 20. Formation of mesoporous materials (I) derived from kanemite; (II) with randomly and (III) with hexagonally ordered channels, along with the corresponding X-ray diffraction patterns [119].

microscopy between the birefringent patterns obtained for the hexagonal POE/water liquid crystal, the synthesis gel (after removal of the methanol hydrolysis product), the as-synthesized product (figure 21) and the calcined product. These observations strongly supported the TLCT theory, where it was postulated that the surfactant forms a liquid crystal phase before the condensation of the silica, and remains in the same phase throughout the synthesis.

Calcination at 500°C of the as-synthesized mesoporous product resulted in a shrinkage of the lattice spacings, but the symmetry of the structure was retained. Polarizing microscopy images of the calcined material were very similar to those obtained for the as-synthesized material.

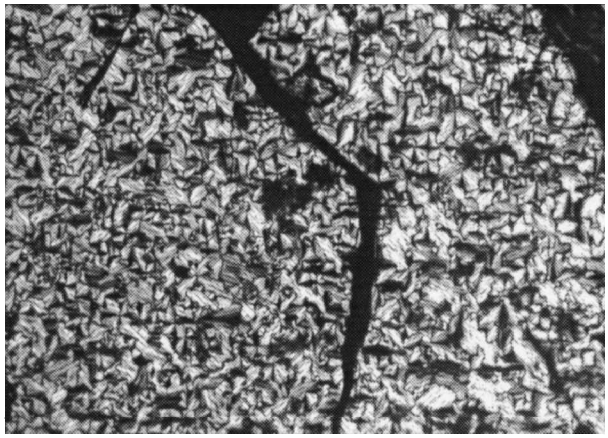

Figure 21. Photomicrograph of the optical texture of the as-synthesized hexagonal mesoporous product synthesized using $C_{12}EO_8$ as the polyoxyethylene surfactant template, as seen by polarizing microscopy (magnification $\times 40$).

Powder X-ray diffraction patterns for as-synthesized and calcined products templated using the $C_{12}EO_8$ POE template are given in figure 22. The product was hexagonal, and calcination had the effect of enhancing the structural regularity of the product. The *d*-spacing for the as-synthesized product was 45 Å; after calcination it was reduced to 38 Å.

Another method used by Attard and co-workers for following the structural evolution of TLCT mesoporous products was deuterium NMR. Evidence was obtained from these measurements to support the assumption that the mesoporous structure is templated directly by the liquid crystal phase [125]. Spectroscopic studies of TLCT mesoporous silica showed the presence of a strongly anisotropic surface, in contrast to MCM-41 which showed no detectable degree of anisotropic surface area [11].

One main advantage of TLCT over the dilute regime M41S synthesis is that by using a preformed liquid crystal phase as the templating medium the difficulty in predicting the topology of the mesoporous products is overcome. The structure of the product is known *a priori* from the binary phase diagram of the surfactant/water system. The presence of inorganic precursor species in the liquid crystalline gel has a relatively small effect on the phase behaviour of the original liquid crystal. The production of methanol from the hydrolysis of TMOS causes the liquid crystallinity of the surfactant–water–silicic acid to be temporarily lost. At this stage the components of the mixture mix homogeneously. Continuous vacuum removes the methanol from the system, allowing the liquid crystalline mesophase, containing hydrolysed silica precursors, to reform.

(*a*) (*b*)

Figure 22. Powder X-ray diffraction patterns obtained using a Guinier camera with a monochromatic line source for (*a*) as-synthesized and (*b*) calcined $C_{12}EO_8$ templated hexagonal silica.

The binary phase diagrams in water for the $C_{12}EO_8$ surfactant and the $C_{16}EO_8$ surfactant are given in figure 23. Attard *et al.* [124] reported the synthesis of a cubic direct-templated structure using the $C_{16}EO_8$ template. Due to the narrow concentration region where the cubic *Ia*3*d* phase exists in the phase diagram, however, it is not as straight forward to obtain the cubic phase as it is to obtain the hexagonal phase. In our experience, room temperature synthesis of the cubic material often resulted in a product consisting of coexisting cubic and hexagonal phases. The TLCT technique is very versatile and can be extended not only to the whole family of non-ionic polyoxyethylene surfactant templates, but also to other ionic surfactant templates.

Calcination at 500°C removed all the organic template from the mesoporous product leaving, in the hexagonal case, a matrix of hexagonally packed 1-dimensional channels, as confirmed by TEM. BET nitrogen adsorption measurements showed that the hexagonal $C_{12}EO_8$-templated calcined product had a specific surface area greater than 1000 $m^2\ g^{-1}$, and a very narrow pore size distribution at 20 Å diameter. These values compared well with the large surface areas obtained for MCM-41, the hexagonal M41S analogue.

The versatility of the synthesis procedure made the synthesis of mesoporous structures other than silica possible. Aluminium silicate was one example of this [125], and later in the review we will discuss the TLCT of mesoporous Pt metal. Probably the most important advantage of the TLCT technique over other precipitation-based routes is that nanostructured monoliths (macroscopic uncracked pieces of material) can

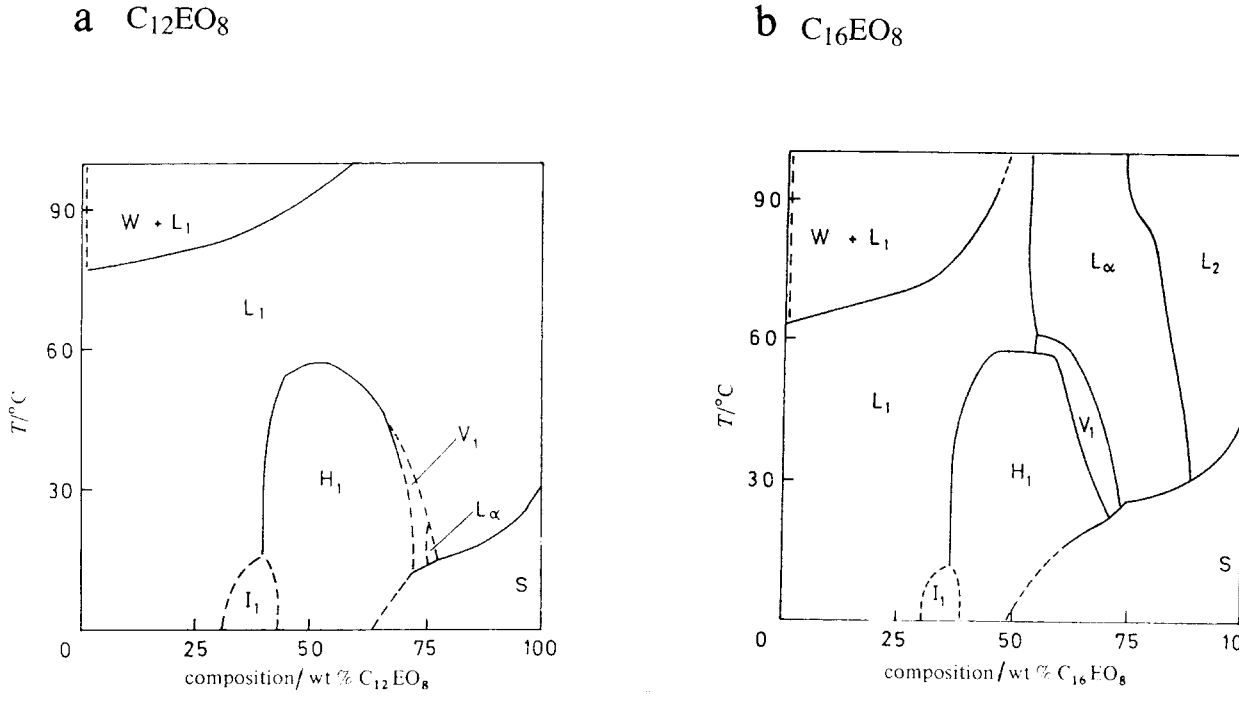

Figure 23. Phase diagrams for (*a*) the $C_{12}EO_8$ surfactant and (*b*) the $C_{16}EO_8$ surfactant in water [126]. L_α, H_1 and V_1 are lamellar, hexagonal and bicontinuous cubic phases, respectively. I_1 is a close-packed spherical micelle cubic phase, L_1 is a micellar phase, S is solid surfactant and W is water. L_2 is a liquid surfactant phase containing dissolved water (only partially miscible). Reprinted with permission from *J. chem. Soc., Faraday Trans.*, 1983, **79**, 975.

be formed. The pore size distribution in the products is strictly unimodal (centred on one value, in the mesoscopic range) and there is no microporosity or interparticle macroporosity.

Attempts have also been made to cast organic polymeric materials using lyotropic liquid crystal structure-directing media. The morphological constraints imposed by the liquid crystal interfaces on the reacting oligomers was however too weak to impede the formation of thermodynamically preferred structures. The cross linked polymeric products from these processes were highly ordered, but their structure did not resemble the morphology of the directing liquid crystalline gel [11].

Recently Weissenberger *et al.* used high molecular weight amphiphilic block copolymers as templates for structured silica [127]. The block copolymers formed 3-dimensional ordered structures in water, which were very stable with respect to temperature and composition, but had no clearly defined liquid crystal phase. Silica polymerization within the aqueous regions of these mesophases led to large nanostructured transparent silica monoliths, with no known liquid crystal phase equivalent. The block copolymer templates were removed by solvent extraction. The resulting structures consisted of bicontinuous arrays of pores with diameters between 8 and 13 nm. The total surface area of the materials was found to be $\sim 500\ m^2\ g^{-1}$.

All of the above-mentioned TLCT synthetic procedures made use of *normal* oil-in-water lyotropic liquid crystal phases as templates rather than *inverse* water-in-oil liquid crystals. Attempts at directing morphology of inorganic products using inverse liquid crystal phases have so far been largely unsuccessful. Gray *et al.*, however, used a polymerizable inverse hexagonal liquid crystal to form a rigid polymer matrix containing aqueous channels [128]. Precursors for the formation of inorganic products were dissolved in the aqueous channels, and reaction of these yielded interesting highly ordered nanocomposite materials. TEOS was used as the silica source, and its polymerization within the mesopores of the polymer matrix was followed by ^{29}Si MAS (magic angle spinning) NMR. The silicate polymerization was poor due to dimensional and diffusion constraints within the mesopores. The composite product contained approximately 2 wt % silica, and was stable to 438°C.

McGrath *et al.* templated a porous silica phase directly from a cetylpyridinium chloride lyotropic L_3 phase using TMOS [129]. The L_3 phase consists of a multiply connected amphiphile bilayer forming a random network, separating the water volume into two subvolumes (figure 24). During synthesis, the surface of the surfactant bilayer was coated with a uniform layer of silica, leaving

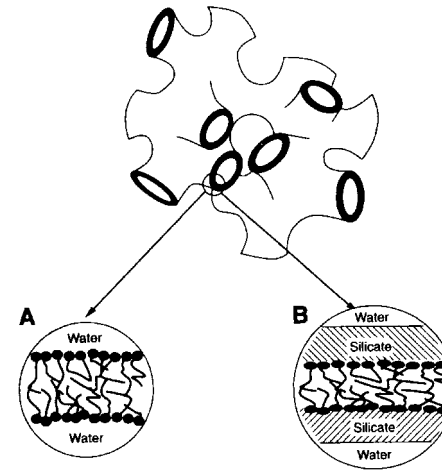

Figure 24. Schematic representation of (A) the surfactant L_3 phase and (B) the silicate L_3 structure [129].

a large proportion of the bicontinuous pore structure free (filled with water). The pore size of the product was controlled by the relative concentration of the surfactant in the L_3 phase, rather than the surfactant chain length. No phase separation took place during the synthesis, which meant that the resulting product was a large monolith. The samples were vacuum-dried at 85°C and degassed at 90°C, without calcination. The two bicontinuous water volumes were therefore void and led to the material having considerable surface area. Had the material been calcined, a third void channel would have been created within the structure, increasing the total surface area of the material. The degassed materials had well defined silica wall thickness and a monodisperse pore dimension (< 80 Å).

All the above work produced monolithic structured inorganic solids with very uniform pore dimensions. The lack of inter-particle porosity or other microporosity makes these materials suitable as matrices for studying the effect of confinement on matter. Frisch *et al.* compared the effect of confinement on polystyrene situated in the pores of mesoporous TLCT silica and in larger amorphous silica nanotubes [130]. A study of the glass transition of the confined polystyrene by differential scanning calorimetry (DSC) showed that no glass transition occurred for the mesoporous silica composite, whilst the normal glass transition was observed for polystyrene confined in the silica nanotubes. It was suggested that in the mesoporous composite, the polystyrene existed as long 1D polymeric strands where the usual glass transition was made impossible by the narrow mesopore dimensions.

True liquid crystal templating (TLCT) can be compared with 'organic matrix mediated biomineralization' where the solid oxides grow on or in a pre-formed

organic matrix. One main advantage of direct-templated mesoporous products over the dilute regime materials is that they can be coated onto objects of diverse shape and size. The resulting coatings remain intact after calcination, as will be described further in §10. TLCT has slightly more in common with biomineralization processes than LCT, because it takes place in small delineated spaces filled with fluid, whilst LCT relies on largely unpredictable heterogeneous precipitation of ordered structures from bulk solution. Biomineralization in living organisms generally occurs in confined membrane-bound areas within cells.

9. Macroscopic morphology control

The alkaline M41S synthesis procedure generally produces very fine particles of mesoporous material, which are suitable for catalysis applications but not for many of the specialized applications outlined at the end of this review. Acidic conditions have become widely used for mesoporous silica synthesis because of the greater control which can be imposed on the macroscopic morphology of the product. The lack of ionic bonds at the silica/organic interfaces for acidic preparations allows more fluidity in the self-organizing system with respect to basic preparations. This effectively makes macroscopic morphology control possible in acidic systems [13].

Virtually all successful work on controlling the bulk morphology of mesostructured M41S-type materials from dilute regimes has used acidic synthesis conditions with pH lower than the aqueous isoelectric point for silicate anions, or has made use of cosolvents such as ethanol. A few rare exceptions of bulk morphology control in basic media were seen for the production of hard mesoporous spheres [131] and for the magnetic field-induced alignment of alkaline-lyotropic silicate–surfactant liquid crystals [132]. For TLCT sol–gel products such as mesoporous silica, moulding the shapes of the products is very straight forward due to the monolithic nature of the resulting materials.

For an acidic mesoporous M41S silica synthesis under aqueous conditions Yang *et al.* reported the formation of a remarkable array of macroscopic shapes, surface patterns and channel arrangements [133]. The reaction conditions favoured curved morphology (toroidal, disk-like, spiral and spheroidal particles). Powder X-ray diffraction showed that the underlying mesostructure for all the morphologies was ordinary hexagonal MCM-41. The proposed initial step for the morphogenesis of these shapes was the formation of a silicate liquid crystal embryo with hexagonal cross-section. This grew over time and depending on the various reaction conditions was subject to different degrees of curvature [133].

9.1. *Monolithic silica films, fibres and spheres*

The aim of producing monolithic macroscopic continuous films of mesoporous silica has attracted the interest of several research groups. Ryoo *et al.* succeeded in producing monolithic hexagonal MCM-41-like films, fibres and plates ($\sim 1\,cm^2 \times 0.5\,mm$ thick), by controlling the degree of silicate polymerization of their synthesis gel by heating under reflux with a non-aqueous solvent [134]. The synthesis gel consisted of TEOS, CPCl surfactant template, water, HCl, ethanol and *n*-heptane. Effectively, the silicate polymerization step of the synthesis was decoupled from the self-aggregation of the surfactant micelles. The synthesis gel was then concentrated using a rotary evaporator. The resulting high viscosity gel was coated in thin films on slide glass, cast in a petri dish, or pulled into fibres via a nozzle equipped with a drying air flow. Any remaining solvent was subsequently evaporated at 313 K.

Depending on the synthesis conditions, the mesoporous product which remained after solvent evaporation contained randomly oriented channels, or channels arranged parallel to the flat external flask surface. The alignment of the channels was proven by X-ray diffraction on the flat films/plates, with the reflecting plane of the X-rays parallel to the flat plate surface. Only the 1 0 0 and 2 0 0 reflections were observed for the aligned hexagonal phase. Treatment of the product with TEOS vapour at 423 K was found to be a useful tool for preventing micro-crack formation. The synthesis gel pH was above the silicate isoelectric point, so it was suggested that the synthesis mechanism was driven by weak non-bonded multipole (non-ionic) interactions. The degree of silicate hydrolysis prior to solvent evaporation was found to affect the silicate–surfactant organization profoundly [134].

Anderson *et al.* used methanol as a cosolvent in the CTAB/TMOS MCM-41 synthesis to produce monolithic periodic mesoporous silica gels and pellets of arbitrary shape and size [135]. The monolithic gels consisted of colloidal particles which in turn contained crystalline domains of hexagonally ordered mesopores. The calcined monoliths were found to be more than 50% porous, partly due to the intra-particle mesoporosity, and partly due to the inter-particle porosity. The porosity was therefore bimodal, consisting of uniform dimension intra-particle mesopores, of which a large fraction were accessible, and a considerable inter-particle porosity. Crack-free periodic silica thin films have been synthesized on non-porous substrates, using a novel method called gas catalysed thin film synthesis (GCTFS) where ammonia was diffused into a homogeneous micellar M41S coating solution on a non-porous substrate. The silica films again consisted of aggregated sub-micrometer colloidal mesoporous particles [136].

The synthesis of mesostructured surfactant–silicate transparent thin films by spin-coating was first reported by Ogawa: a hydrothermally unstable lamellar product was produced [137]. More recently the same technique has been applied to a novel acid-catalysed synthetic method, which produced thin films of mesoporous MCM-41 [138]. The novel synthesis consisted of adding the alkyltrimethylammonium template to a pre-hydrolysed TMOS gel prior to spin-coating and silicate polymerization. XRD patterns of the film gave no indication of alignment of the mesostructure. Synthesis gels containing pre-hydrolysed tetramethoxysilane and alkyltrimethylammonium bromide surfactants were used to synthesize transparent composite coatings consisting of aggregates of surfactant and thin silica layers. The d values of the products varied depending on the relative ratios of tetramethoxysilane and surfactants used [139, 140].

Lu *et al.* produced continuous mesoporous silica films with 2D hexagonal and cubic ($Pm3m$) symmetries under acidic conditions by dip-coating [141]. The synthesis gel composition and synthesis conditions were optimized, producing high quality crack-free films with the desired thickness and phase. It was shown by surface acoustic wave measurements (SAW) that the mesoporosity in the films was fully accessible to molecules from the gas phase. The $Pm3m$ cubic phase had not previously been reported for either liquid crystalline phases or water–surfactant–silica systems.

Bruisma *et al.* have synthesized mesoporous spun silica fibres and hollow spheres by fast solvent evaporation of hydrolysed alkoxysilane/cationic surfactant solutions under acidic conditions [142]. The spinnable synthesis solution consisted mainly of ethanol, with a small quantity of poly(ethyleneoxide). The spun fibres had highly ordered hexagonal channels aligned parallel to the fibre axis.

Mesoporous transparent solid silica spheres with various diameters (50 μm–2 cm) were selectively produced via an emulsion chemistry route using tetrabutyl orthosilicate (TBOS) as the silica precursor, and cationic alkylammonium surfactant template species [131]. The pores were shown by TEM and nitrogen absorption studies to be of uniform size, with total surface area over 1000 $m^2\ g^{-1}$.

Very small spheres of MCM-41 were synthesized using an alkaline ammonia/ethanol/*n*-hexadecylpyridinium chloride surfactant system, where the shape and size of the particles can be assumed to be controlled by the emulsion environment [143]. The product particle size was controllable within the range 400–1100 nm. Under specific pH conditions, Yang *et al.* found that for the acidic M41S synthesis, spheres of mesoporous silica were favoured over the usual gyroid product morphology [144]. The gyroid structures involved fast and local polymerization of growing silicate liquid crystal seeds, whilst the sphere morphology was favoured for the slower global polymerization of a silicate liquid crystal droplet. Surface tension was suggested to cause such a droplet to adopt a spherical shape, and ultimately to be rigidified as a mesoporous silica sphere.

10. Synthesis of oriented films of mesoporous silica

10.1. *Alignment at interfaces*

Yang *et al.* have described two methods for orienting the channels of mesoporous silica synthesized from a dilute regime acidic CTACl-templated system (the SiO_2 precursor was TEOS) [145, 146], figure 25. The first method involved introducing into the synthesis gel a freshly cleaved mica surface on which elongated islands of aligned mesoporous silica were seen to grow over periods of hours to days. Mica appears to influence the preferred direction of growth of the hexagonal channel structure. Brick-like distortions in the channel shape are seen at the mica interface in the TEM image in figure 26. This can be taken as evidence for the strong interaction between the synthesis gel and the mica. The mesoporous films adhered quite strongly to the mica surface, even after calcination.

Yang *et al.* also obtained mesoporous silica continuous film growth on cleaved pyrolytic graphite using an acidic synthesis gel (containing CTACl and TEOS) [147]. The mesoporous channels aligned along any of the three symmetry-equivalent (C_2) axes of the hexagonal graphite substrate, parallel to the graphite surface. It was proposed that the film growth mechanism was initiated by a thin liquid crystal surfactant–silicate film with aligned hemi-micelles at the graphite surface.

The alignment of adsorbed surfactant molecules at the interface between water and amorphous silica, mica and graphite substrates has been observed using a pre-contact mode electric double layer (EDL) AFM soft imaging technique [148–150]. Alignment of surfactant tubules was seen at mica and at graphite surfaces, but a random arrangement of surfactant tubules was seen at the amorphous silica interface. Attractive interactions between the graphite surface and the surfactant tails were claimed to be responsible for the horizontal adsorption of surfactant molecules, leading to a first layer of hemi-micelles which in turn induced a very strong orienting effect on the rest of the adsorbed surfactant film. The hydrophilic mica surface was found to attract surfactant head groups, orienting the molecules perpendicular to the interface. This led to the first layer of surfactant micelles having a smaller interaction area with the mica surface than with the hydrophobic graphite surface. Mica was seen to have a slightly weaker orienting effect

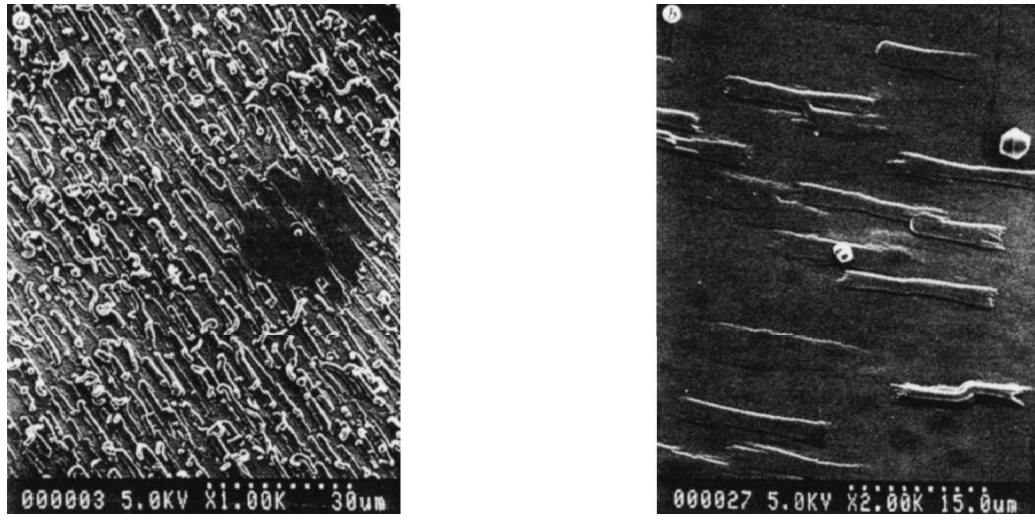

(*a*) (*b*)

Figure 25. (*a*) SEM micrograph showing the initial small oriented crystals of mesoporous silica (nucleation stage), with a preferred alignment. (*b*) SEM micrograph of mesoporous silica film after calcination (after several days gel ageing). Preferred alignment is visible [145]. Reprinted with permission from *Nature*, 1996, **379**, 703. Copyright 1999 Macmillan Magazine Limited.

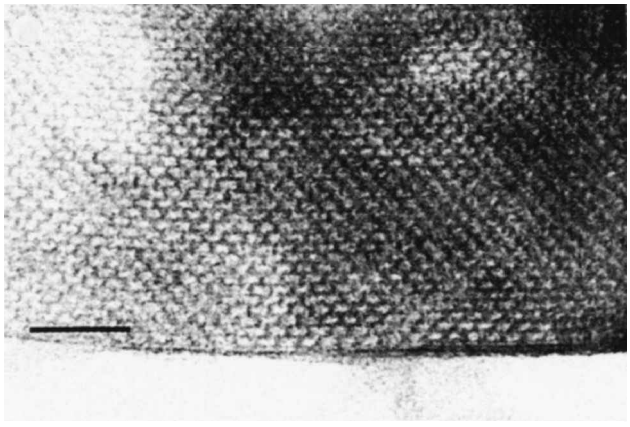

Figure 26. TEM image of the calcined material. At the mica interface, brick-like distortions in the mesopore shape are visible (scale bar, 25 nm) [145]. Reprinted with permission from *Nature*, 1996, **379**, 703. Copyright 1999 Macmillan Magazine Limited.

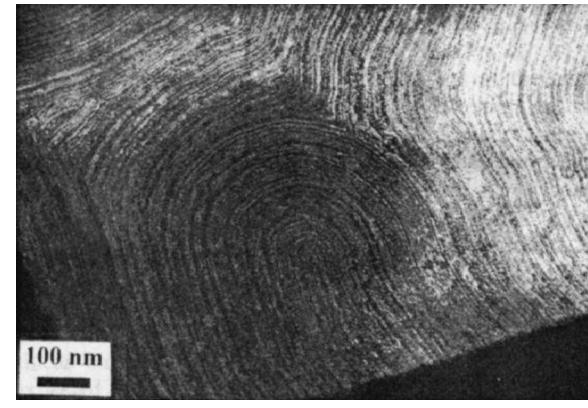

Figure 27. TEM image of the channel pattern for a sample of mesoporous film grown at the boundary between air and water showing a curved mesopore arrangement created due to constraints on packing in the film [151]. Reprinted with permission from *J. mater. Chem.*, 1997, **7**, 1755.

on the adsorbed liquid crystal phases than graphite [148].

Alignment was also observed for a mesoporous film synthesized at the air–water interface. The channels again aligned parallel to the surface of the film [146]. This time, however, the films were free-standing and could be easily isolated. The presence of an external interface can restrict silica–surfactant self-aggregation causing local frustrations to arise. The transformations which occur to relieve such packing stress lead to very interesting mesopore formations, as shown in the TEM micrograph in figure 27 [151]. These transformations are assumed to occur before the silicate is fully polymerized, and relieve stress through rotational displacements of the surfaces (disclination effects).

X-ray reflectivity measurements during mesoporous film synthesis at the air–water interface have shown that the mechanism for film growth consists of two steps [152]. Firstly an organized surfactant layer forms at the interface, in the first 10 h of reaction. When the interfacial surfactant layer is complete (thickness $\sim$30 Å), the silicate polymerizes rapidly within the layer, forming the regular mesoporous film structure.

Yang *et al.* later demonstrated that the film growth, defect structure, extent of polymerization, and mesoporosity sensitively depended on the choice of synthesis

acidity, temperature and mixing, and in the case of supported films, on the choice of substrate [153]. A ten-fold increase in the thickness of as-synthesized films was obtained by simply lowering the acidity and using ambient temperature conditions. The observation of a focal-conic fan-type texture in the free-standing films showed that defect-controlled director fields, that exist in precursor hexagonal lyotropic silicate mesophases, were preserved in the channel structure of the mesoporous silica phase. The liquid crystal-like optical textures observed for free-standing mesoporous silica films were taken as evidence for the self-aggregation of surfactant–silica mesophases prior to silicate polymerization.

A further development in the dilute regime field has been described where mesoporous structures are templated at an oil–water interface [154]. Spherical shells of both 2D hexagonal ($p6mm$) and 3D hexagonal ($P6_3/mmc$) mesoporous material were produced in stirred oil-in-water emulsions, and thin homeotropically aligned films of mesoporous material (channels perpendicular to the film) were produced at static water–oil interfaces. The mesopores in the spherical shells were mainly radially oriented. The schematic diagram in figure 28 shows the proposed mechanism of formation for these oriented films. The synthesis mixtures were acidic and the silica precursor, TEOS, dissolved in the oil phase of the emulsion. The surfactant molecules were highly concentrated at the oil–water interface, and this was where the mesoporous composite material formed.

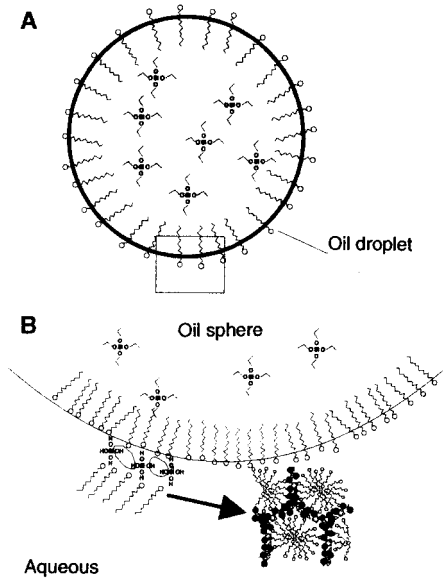

Figure 28. Schematic drawing of the suggested formation of the mesoporous spheres. (A) The oil droplets in the emulsion contain dissolved TEOS; the emulsion is stabilised by surfactant molecules at the oil-water interface. (B) Area of A expanded; TEOS is hydrolysed at the oil/water interface and solidifies into the mesoporous product. The morphology of the final product is moulded on the original oil droplet [154].

Oil–water two-phase systems have been used to synthesize long optically transparent mesoporous silica fibres [155]. Initially a mesoporous silica film formed at the water–oil interface, and mesoporous fibres grew progressively into the aqueous phase of the two-phase system. On the oil side of the film ball-like structures with diameters of $\sim 100\,\mu m$ were observed. Depending on the pH and hydrolysis rate of the synthesis gel, a variety of other silica shapes was seen on the aqueous side of the film: toroidal, disk-like, spiral, hexagonal, rope-like, discoid, pinwheel, gyroid, bagel, sheet, clock, eccentric. When TBOS was used as the silica source, the organic second phase was not necessary for the formation of the mesoporous silica fibres. Long optically transparent fibres, from $100\,\mu m$ to 5 cm long, with hexagonal or circular cross sections of $1–10\,\mu m$ diameter were obtained. Well ordered hexagonal arrays of long mesopores running parallel to the fibre length were seen by TEM [155].

The drawback with most interfacially aligned hexagonal mesoporous products described so far is that the mesopores tend to lie parallel to the substrate. The access to the mesopores is therefore greatly restricted. Tolbert *et al.* overcame this problem by synthesizing 3D hexagonal ($P6_3/mmc$) mesoporous silicate thin films using gemini quaternary ammonium surfactants as surfactant templates under acidic conditions [156]. It was suggested that the mesoporous material nucleated on hexagonally close packed (hcp) surfactant micelles. The films were grown on mica and at the air–water interface and were very well aligned, with the c-axis of the phase perpendicular to the external surface [156]. The use of micellar cubic phases is presently being investigated for TLCT systems, and has already provided some encouraging results [157].

A novel means of introducing patterns and thin film motifs into mesoporous silica films was presented recently by Ozin and co-workers [158]. A combination of self-assembled-monolayer (SAM) lithography and mesoporous silica chemistry was applied under acid synthesis conditions to produce linear arrays of oriented silica particles on alkanethiol decorated gold surfaces that had been patterned with polydimethylsiloxane stamps.

10.2. *Alignment due to shear*

In a very recent paper, Edler *et al.* have reported that alkaline MCM-41 synthesis gels containing high KBr concentrations can be aligned under shear [159]. The concentration of KBr is critical, however, because its presence can disrupt the silica condensation process at

high concentrations. It also affects the *d*-spacing of the resultant material. Synthesis gels without KBr showed no alignment due to shear.

Hillhouse *et al.* used a purpose-made continuous flow reactor to show that external flow can induce preferred hexagonal mesophase orientation in thin films [160]. During the first two hours of synthesis, growth proceeded, on average, more along the flow direction and less in transverse directions. The morphology of the products suggested that the growth of the films proceeded with layer-by-layer deposition rather than via the deposition of pre-formed particles.

10.3. *Alignment induced by electric and magnetic fields*

By infiltrating an MCM-41 synthesis gel into the microcapillaries of a mould in contact with a substrate, it has been possible to direct the growth of aligned tubules via electro-osmotic flow induced by an electric field applied tangentially to the substrate surface [161]. The electro-osmotic flow was also found to enhance the rate of silica polymerization around the tubules by localized Joule heating. After removal of the mould, patterned bundles of oriented nanotubules remained on the substrate surface.

Firouzi *et al.* macroscopically oriented alkaline silicate–surfactant non-condensed liquid crystal phases by heating the mixtures above their anisotropic to isotropic transition temperature and then allowing them to cool in a magnetic field [132]. Different orientations of the liquid crystal phases were obtained when using different organic cosolvent molecules in the mixtures. The field-aligned hexagonal silicate–surfactant liquid crystal was then allowed to solidify by silicate polymerization. Calcination produced macroscopically oriented hexagonal mesoporous monolithic products [162].

10.4. *Alignment of TLCT materials*

Our own work on the alignment of direct-templated mesoporous films on mica or glass has not given any conclusive evidence that the TLCT films are affected by the substrate. A fibre average alignment, with the mesoporous channels of the material randomly arranged in the plane of the surface, was observed. Confinement of the synthesis gels within a mica sandwich was also unsuccessful due to the build-up of methanol, which ultimately disturbed the liquid crystal template, leading to amorphous products. Confinement of the synthesis gels in very narrow open-ended capillaries, however, gave very interesting results [163]. Highly aligned mesoporous monolithic coatings (without cracks) were produced on the inside of the capillaries (see figure 29).

The alignment of the mesopores within the coatings was seen by X-ray diffraction, and it was postulated that the hexagonally packed channels of the coating were arranged in rings, or a spiral against the walls of the capillary. After calcination at 500°C the coating remained intact, and X-ray diffraction showed that the underlying hexagonal aligned structure was not disturbed. In fact, as shown in figure 29(*c*), there were more orders of diffraction observed for the 6-spot aligned X-ray pattern than prior to calcination. An *in situ* X-ray analysis of the kinetics of the capillary alignment showed (figure 30) that the hexagonally structured coating formed very quickly once the methanol was removed from the gel. The aligned 6-spot pattern formed immediately, with no disordered intermediate powder pattern being seen.

The alignment of these coatings is thought to be mainly due to the effects of gel confinement in such a small volume. The nature of the walls of the capillary, however, is also very important for the alignment process. When the capillary walls were rendered hydrophobic by treating the quartz capillary with phenyltrimethoxysilane (PhTMOS) prior to introducing the synthesis gel, a disordered mesoporous coating resulted.

As a support for active catalytic sites, this aligned material may have interesting selectivity with respect to other non-aligned materials, or it may find uses in advanced separation technology. Capillaries containing these aligned mesoporous coatings may find interesting applications in the field of capillary electrophoresis, and this potential is being assessed in the Analytical Chemistry Section at Imperial College, London.

11. Biomimetic strategies

Biomineralization in living organisms results in the formation of elaborately designed crystalline and amorphous structures, with beautiful symmetry and ultrastructure [164]. In the fields of biological systematics and palaeontology, the evolution of bioinorganic structures has long been a main subject of study. However, the chemical and biochemical processes controlling biomineralization have only more recently come into the limelight of research. Parallels between biomineralization, as seen in Nature, and liquid crystal templating, have been noted by many workers in the field of LCT.

It is believed that by mimicking mineralization processes occurring in living creatures, we will gain access to a whole new range of functional inorganic structures. Recently concepts such as morphogenesis (synthesis with structure-direction), replication, self-assembly and metamorphosis have become very useful in devising innovative strategies for materials synthesis. Complex inorganic materials, of which mesoporous materials are a key example, can be chemically synthesized by pattern replication of self-organized organic assemblies, such as micelles, vesicles and foams [165].

Tiny sea creatures such as radiolarians and diatoms form (figure 31) fascinating protective shells of amorphous

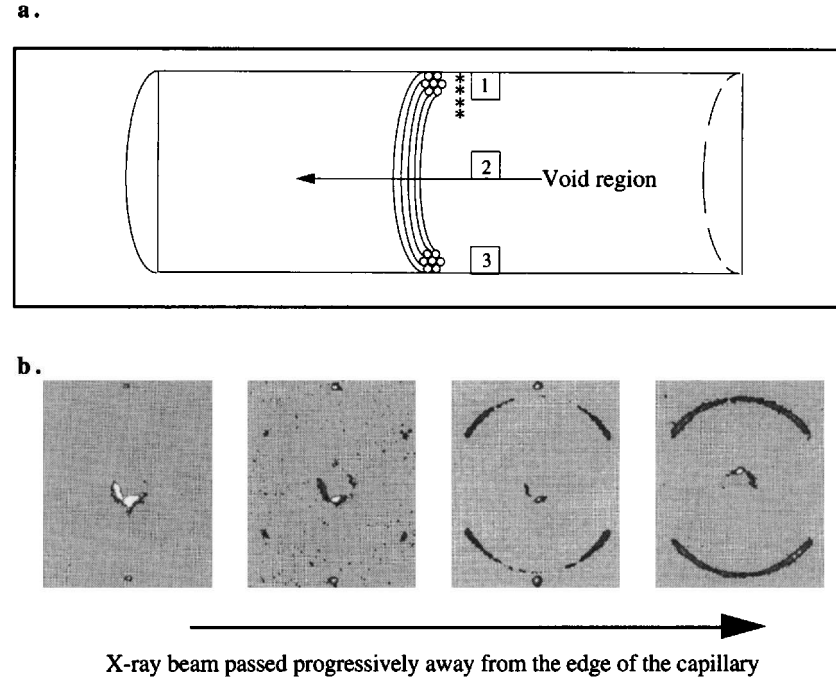

Figure 29. (*a*) Schematic longitudinal section of a coated capillary showing hexagonally packed channels of mesoporous SiO_2/C_nEO_8 product lining the capillary walls ($n = 10$ or 12). 6-spot patterns were obtained when the X-ray beam was passed perpendicularly through the capillary at positions (1) and (3); no diffraction pattern was obtained when the X-ray beam was passed through the centre of the capillary (2). (*b*) Sequence of X-ray diffraction patterns obtained for the aligned $SiO_2/C_{10}EO_8$ composite coating when the X-ray beam crossed the capillary at positions shown by asterisks in part (*a*). (*c*) Pattern obtained for the calcined sample when the X-ray beam was passed through the edge of the capillary [163]. Reprinted with permission from *J. chem. Soc., Chem. Commun.*, 1997, 1843.

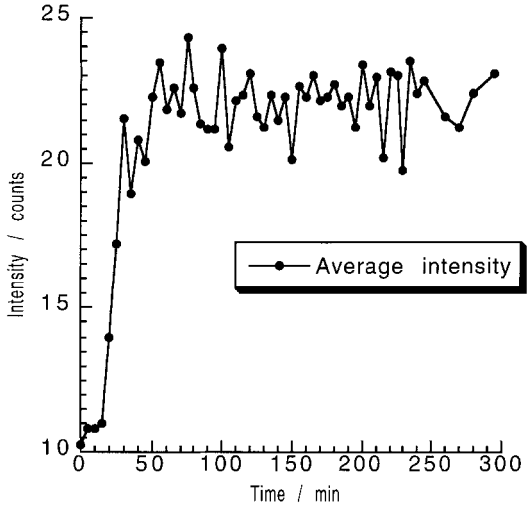

Figure 30. Plot of average diffraction spot intensity versus time for an *in situ* X-ray diffraction experiment to probe the kinetics of the alignment process [163]. Reprinted with permission from *J. chem. Soc., Chem. Commun.*, 1997, 1843.

silica, through a biologically induced mechanism which involves the use of organic templates. This example of biomineralization has rather strong parallels with LCT, which uses self-assembled surfactant phases as templates to produce ordered structures with amorphous walls. LCT can therefore be ranked as a *biomimetic strategy* [148].

The micro-organism kingdom of the protocista (Eukaryotes) form several different amorphous mineral types, commonly with calcium and silicon. Six protocist phyla use a unique process to make their protective shells, where mineralized 'building blocks' are formed intracellularly and are then transported to the cell surface where they are assembled. This vesicular mechanism sets these phyla apart from all other eukaryotic kingdoms. The synthesis of lamellar aluminophosphates and hollow aluminophosphate microspheres with surface patterns similar to those of diatom and radiolarian microskeletons has also been reported [167, 168] (see figure 32).

In a more general article Ozin and Oliver proposed a templating model based on surfactant vesicles similar to those in cells to explain the macroscopic forms and

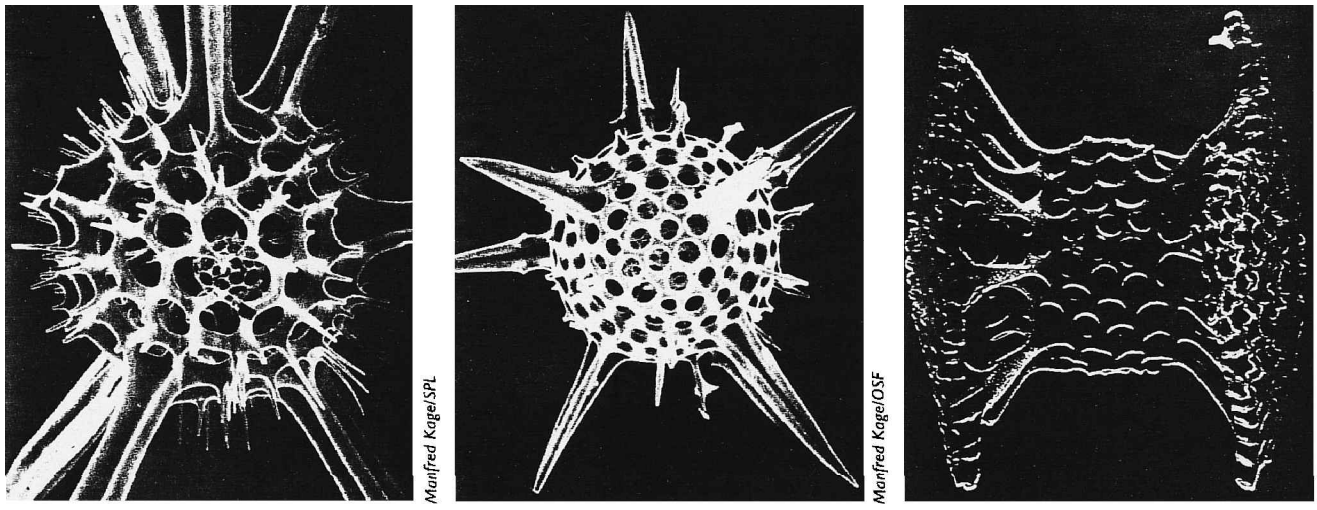

Figure 31. Patterned shells of microscopic sea creatures [166].

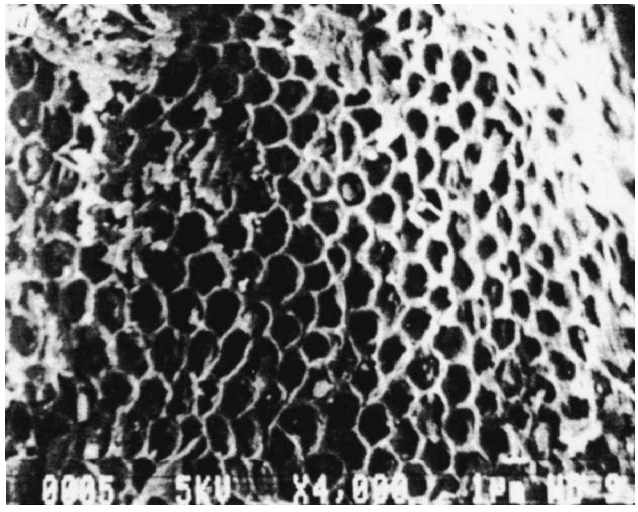

Figure 32. Scanning electron micrograph of the decylamine-templated mesolamellar aluminophosphate product, showing the 1 μm honeycomb surface morphology [167]. Reprinted with permission from *Nature*, 1995, **378**, 47. Copyright 1999 Macmillan Magazines Limited.

surface patterns of their aluminophosphate composite ultrastructures [169]. The mineral products moulded themselves to the surface morphology of the vesicle. Further articles describing the morphosynthesis of biominerals similar to bones and shells and generally extending the notions to the production of synthetic materials have also been published over recent years [170–173]. Synthetic biomaterials, such as artificial bone, are of critical importance for biomedical applications such as for surgical implants.

A surface textured lamellar aluminophosphate material has been templated using phosphate surfactants with the formula $[C_nH_{2n+1}NH_3^+][H_2PO_4^-]$, where $6 \leqslant n \leqslant 18$ [174]. These liquid crystal phases were found to have interesting surface textures when observed by polarizing microscopy. The mineral was prepared organo-thermally, in polyethylene glycol-based organic solvents rather than in the aqueous regions of a lyotropic liquid crystal phase, from aluminium oxide, phosphoric acid and *n*-alkylamines. The lamellar aluminophosphate replica materials emerged with surface textures similar to the original liquid crystal phase, and were therefore said to have biomimetic form.

A method for synthesizing hollow porous shells of crystalline calcium carbonate (aragonite), that resemble the coccospheres of certain marine algae has also been described [175]. Micrometer-sized polystyrene beads were used as the substrate around which the calcium carbonate shells formed. The pore size in the resulting honeycomb inorganic structure was determined by the relative concentrations of water and oil in the synthesis mixture.

Elaborately structured biosilicates also exist in Nature, and come a step closer to the M41S family. Biopolymers containing anionic and hydrogen-bonding functionalities, which are likely to have a structure-directing role, have recently been found in biosilicates. In their paper describing biosilicates and biomimetic silicate synthesis, Zaremba and Stucky [176] point out the increased use of biomineralization techniques, mild reaction conditions, biogenic and biomolecule-like organic dopants, and biosilicate starting materials in the laboratory synthesis of functional silica materials such as MCM-41.

A biomimetic templating approach to the synthesis of lamellar silicas was described by Tanev and Pinnavaia [177, 178]. The procedure, depicted in figure 33, was based on the hydrolysis and condensation of a neutral silicon alkoxide precursor, in the inter-layer regions of the multilamellar vesicles formed from neutral diamine

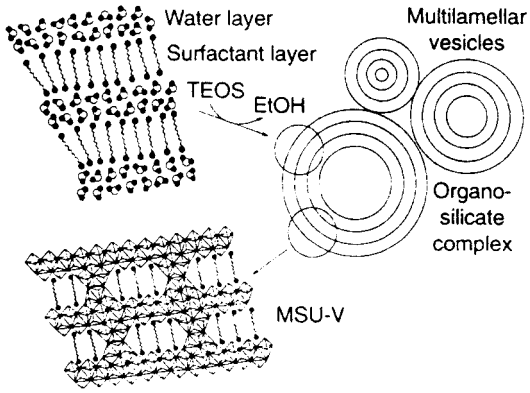

Figure 33. Proposed biomimetic vesicular templating mechanism of the formation of MSU-V [177].

bola-amphiphile molecules. Thermally stable porous lamellar silicas (MSU-V) with vesicular particle morphology were formed for bola-amphiphile templates of various chain-lengths. Their sorptive properties were found to be similar to those of pillared lamellar silicas.

By carefully controlling the surfactant/water contents and the rate of condensation of silica at high pH, mesoporous MCM-41 tube-shaped structures have been synthesized [179]. The walls of these tubes consisted of hexagonally packed coaxial cylindrical pores (see figure 34). The structures are very similar to structures which occur in Nature (marine diatoms).

The use of self-assembled lipid tubules has also been described for organizing silicon and iron oxides [180]. The sugar-based lipid galactocerebroside, doped with small amounts of an anionic sulphated derivative, was found to induce the nucleation of magnetic and non-magnetic iron oxides. The lipid–iron oxide composites could be synthesized as tubes or lamellar discs depending on the synthesis conditions. Results suggested that the variety of mesostructures formed by chemically modified lipids may provide a route to the production

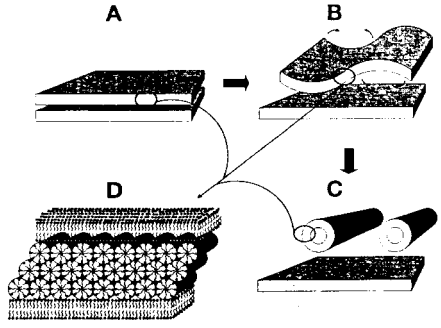

Figure 34. Proposed mechanism for the formation of the microtubular morphology of MCM-41. (A) Mixed lamellar-hexagonal membrane phase; (B) acidification leads to membrane curvature; (C) neutralisation bends the membrane into tubules; (D) the membrane consists of a hexagonal array of cylindrical micelles [179].

of mineral-containing fibres and other ceramic–organic composites.

Recently a fibrous bacterium, *Bacillus subtilis*, was the substrate used for the deposition of an MCM-41-type material [181]. The mesoporous material mineralized in the interbacterial-thread spaces. When the bacteria were removed from the composite material by calcination at 600°C a macroporous structure consisting of mesoporous silica was produced. This method therefore produces materials with porosity in both the mesoscopic (20–100 Å) and macroscopic (0.5 μm) ranges.

12. Applications of mesoporous molecular sieves

The very large surface areas of mesoporous materials make them particularly suitable for applications as catalysts or catalyst supports. The regularity of the pore size within the structures makes them potential candidates for size-selective catalysis applications, cf. zeolites. Their large pore size could make these materials interesting for petrochemical and fine chemical processes involving large molecules.

The sorptive properties of MCM-41 have been characterized for a variety of adsorbates including argon, nitrogen, oxygen, water, alcohols, cyclopentane and benzene [182–190]. The shape of the isotherm was highly dependent on factors such as material composition, pore size and nature of the adsorbent, but type IV isotherms were obtained in almost every case for materials synthesized using the dilute regime method. In general, data confirm that MCM-41 has a narrow pore size distribution and exhibits very large volumes with respect to classical microporous materials.

It should be noted that type IV isotherm behaviour requires the adsorbate to have a high partial pressure in the gas phase. For an industrial application such as volatile organic compound (VOC) uptake, the partial pressures involved are low and would therefore require a material with a type II adsorption isotherm. Nitrogen adsorption BET measurements on TLCT silica produce a type I isotherm (figure 35) which means that low partial pressures are sufficient for adsorption of nitrogen into the mesoporous structures. This property may make TLCT materials advantageous over mesoporous products synthesized in the dilute regime for certain applications.

12.1. *Functionalization for catalytic applications*

Much work has been directed towards the introduction of transition metals into mesoporous materials. Transition metal oxides have variable oxidation states and can therefore be used in tailoring catalytic, electronic and magnetic properties of materials. Pure aluminium and silicon oxides are catalytically virtually inert. In this section we will provide a brief overview of the work

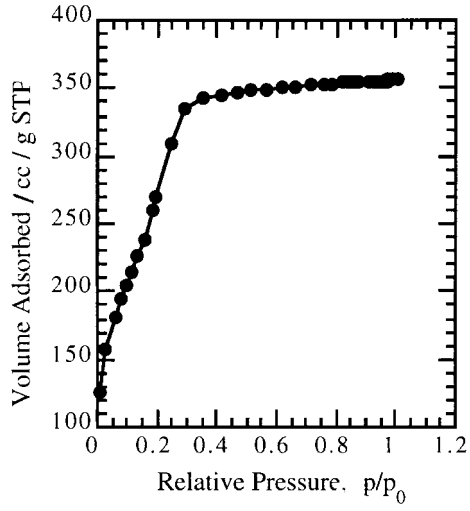

Figure 35. BET adsorption isotherm obtained for nitrogen on calcined $C_{12}EO_8$ direct-templated hexagonal mesoporous silica.

carried out on incorporation of catalytic sites into mesoporous materials. Most of the papers published over the last two years have been concerned with this side of mesoporous materials research, and comprehensive reviews are already available covering this subject [3, 9, 12].

Siliceous solids can be functionalized for catalysis applications by framework substitutions, or activated by post-synthetic surface derivatizations. Mesoporous matrices show great promise in avoiding the limitations due to the small pore size in traditional zeolites. Due to the metastable nature of the mesoporous materials concerned, the surface derivatization method of activation is generally preferred. The four possible methods of derivatization are as follows [3].

(1) Primary modifications: direct grafting of active sites onto the surface silanol groups of calcined or solvent extracted materials.
(2) Second and higher order modifications: grafting onto previously functionalized surfaces.
(3) One-pot synthesis of functionalized mesoporous silica.
(4) Transformation of materials prepared under conditions (1) to (3) by further treatment such as heating, evacuation, calcination and/or reduction.

Transition metals incorporated into the MCM-41 framework or grafted to the MCM-41 surface include titanium [191–195], platinum [43, 95, 196–198], vanadium [199–201], manganese [202–204], boron [205–207], aluminium [90, 92, 94, 97, 208], zinc [209], zirconium [207, 210], binary lanthanum oxides (Na/La, K/La, Rb/La, Cs/La) [211], cobalt [212, 213], ruthenium [214], Ni-Mo clusters [215] and Sn-Mo clusters [216]. In these systems MCM-41 is often used as a host for encapsulating and anchoring organometallic complexes, which may then be decomposed into metal clusters at elevated temperatures.

A novel means of introducing metal ions into mesoporous structures is to use surfactant templates with organometallic complex head groups. Kevan and co-workers used a surfactant with Cu(II) ions coordinated to a macrocyclic cage head group to template the formation of MCM-41 [217]. Surfactants with ferrocenyl head groups have also been used as templates [218]. In our own work, we are investigating the use of surfactant templates with ruthenium complex head groups for the TLCT of mesoporous silica.

Other approaches to functionalizing mesoporous silica include the incorporation of heteropolyacids such as $H_3PW_{12}O_{40}$ into the mesopores of MCM-41 materials [219–221]. Burkett *et al.* discovered that the co-condensation of TEOS with organosilanes in the presence of a surfactant template leads to the synthesis of organically functionalized mesoporous silicas [222]. The organic moiety was covalently linked to the silica walls, and the number of organic sites and the organic loading were easily adjustable by varying the composition of the synthesis mixture. Other research groups have also been investigating means for introducing organic active sites into mesoporous hosts [223–225].

For TLCT systems, the one-pot synthesis of functionalized silica is in theory quite straight forward. The key criterion which determines whether a particular synthesis gel will successfully produce a mesoporous structured catalyst is simply that the addition of the functional moiety does not disturb the liquid crystal template.

12.2. *Synthesis of purely non-siliceous mesoporous solids*

Early attempts to prepare pure transition metal oxide analogues of MCM-41 employed trialkylammonium bromide surfactants as templates in a one-pot procedure and led to the synthesis of W, Pb, Sb, and Fe oxides [29, 52, 60, 226]. Subtle variations of pH and surfactant–metal oxide ratios led to cubic and layered phases. The materials were not, however, stable to surfactant removal (by calcination). Vanadyl phosphate was also synthesized but was again thermally unstable [227].

Papers describing the synthesis of pure transition metal analogues of MCM-41 materials, M-TMS-1 (where M is Nb, Ta or Ti) have been published over the last few years [5, 228–231]. Antonelli *et al.* [231] have used two approaches:

(1) Using soluble and reactive metal alkoxides as precursors for the metal oxide framework.

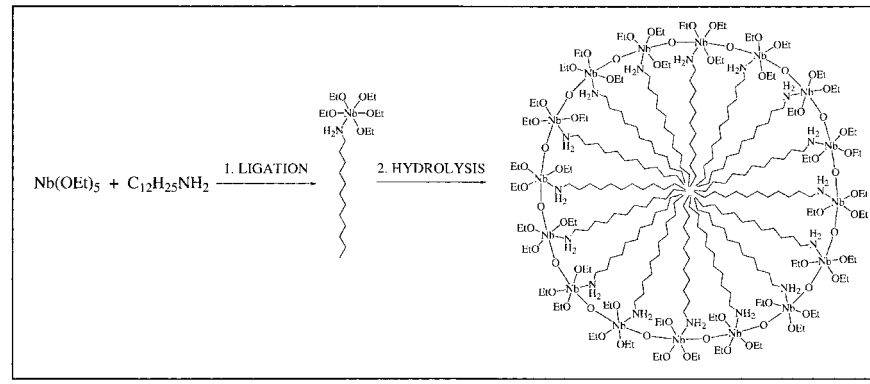

Figure 36. Ligand assisted templating of Nb-TMS-1 [5].

(2) Ligation of the surfactant head group directly to the metal oxide prior to hydrolysis and condensation reactions. This approach is called ligand assisted templating (LAT).

A purely titanium oxide analogue of MCM-41, Ti-TMS-1, was synthesized using the first of the two approaches. Acetyl acetone was used to slow down the hydrolysis reaction of the titanium alkoxide, so that the transition metal oxide could achieve the appropriate interaction with the phosphate head groups of the surfactant [231]. The resulting mesoporous solid was reasonably stable to calcination, but some collapse of the structure occurred, and some of the surfactant was still present after the calcination. Surface areas up to 200 $m^2\ g^{-1}$ were obtained.

Nb-TMS-1 was synthesized by the LAT mechanism, as depicted in figure 36. The removal of the surfactant in this process was fully optimized, and led to high surface area materials which were thermally stable [230]. Nb-TMS-1 also formed the largest crystals (by almost three orders of magnitude) ever reported for any mesoporous material synthesized in a dilute regime; cubic and layered structures were also seen [228].

Ta-TMS1 was the most stable mesoporous transition metal oxide of that series [229]. It was found to have thermal stabilities rivalling that of siliceous MCM-41. In general, the niobium and tantalum oxide molecular sieves were found to have surface areas up to 600 $m^2\ g^{-1}$ and thermal stabilities from 300 to 800°C. The surfactant in the LAT synthesis is removed by acid washes, therefore avoiding the risky calcination step. LAT was recently used by Stone and Davis to synthesize mesoporous titania and niobia [232]. The photocatalytic properties of the materials were assessed.

Ulagappan and Rao attempted the synthesis of mesoporous phases based on SnO_2 and TiO_2, using anionic AOT and neutral primary amines as templates, respectively [233]. Neither mesoporous product was stable to calcination.

Pure zirconia mesoporous materials have also been of synthetic interest recently. Lamellar and hexagonal composite ZrO_2–surfactant phases were synthesized by Reddy and Sayari using primary alkylamines and quaternary ammonium surfactants, respectively [234]. Zirconium sulfate was used as the precursor for the zirconium oxide. The composite materials were not, however, stable to calcination. More successful attempts at producing mesoporous zirconia were described by Ciesla *et al.* [235]. One zirconium source used was $Zr(SO_4)_2.4H_2O$, and CTAB was used as the template. The resulting mesoporous material was similar in structure to MCM-41 (hexagonally packed channels), see figure 37. The structure was stabilized by treatment with phosphoric acid (uncondensed Zr–OH groups react with the phosphate ions which favour completion of the polymerization process). The material was then stable to calcination, though there was a considerable shrinkage of pore size. A different approach was to

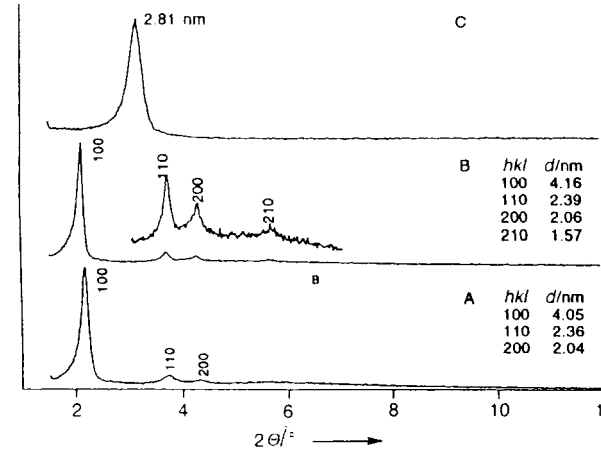

Figure 37. XRD pattern of the zirconium oxide compound synthesized with zirconium sulfate as the Zr source. As-synthesized, containing surfactant (A); after treatment with phosphoric acid (B); and sample after calcination at 773 K (C) [235]. Reprinted with permission from *Ang. Chem. int. Ed. Engl.*, 1996, **35**, 541.

use zirconium propoxide as the ZrO_2 precursor, with strongly acidic CTAB solutions as templating media. The addition of $(NH_4)_2SO_4$ was necessary to reduce the reactivity of the zirconia precursor in the aqueous solution. Again both as-synthesized and calcined materials were mesoporous (hexagonal symmetry), see figure 38.

Thermally stable mesoporous hafnium oxide was recently synthesized via a LCT route; this has potential for use in strong acid catalysts [236]. A vanadium phosphate (VPO) mesoporous material was synthesized by Doi *et al.,* by the intercalation of lamellar $VOHPO_4.0.5H_2O$ with surfactant [237]. Subsequent hydrothermal treatment yielded a product with hexagonal symmetry. Mesoporous manganese oxides stable to 1000°C are another outstanding example of LCT of non-silica materials [238].

Another variation on the above theme of synthesizing catalytically active transition metal mesoporous frameworks was provided by Braun *et al.* [239]. Stable cadmium sulphide and cadmium selenide semiconductor superlattices were templated by surfactant aggregates. These materials were reported to have photosynthetic and photocatalytic applications.

Göltner and Antonielli have extended their TLCT experimental procedures to the synthesis of purely non-siliceous direct-templated mesoporous materials [11]. The lyotropic non-ionic liquid crystal medium was found to be a suitable medium for precipitation and *in situ* redox processes. This property led to the formation of mesostructured, high surface area platinum metal [240]. A regularly structured metal colloid was produced in the aqueous regions of the $C_{16}EO_8$(‡) liquid crystal by *in situ* chemical reduction of a metal salt. The small colloidal particles then agglomerated and coalesced, forming mechanically stable mesopore walls. The resulting material was a coarse powder with particle sizes of 0.1–0.5 μm diameter. The surfactant was removed by solvent extraction yielding uniform 3 nm cylindrical pores.

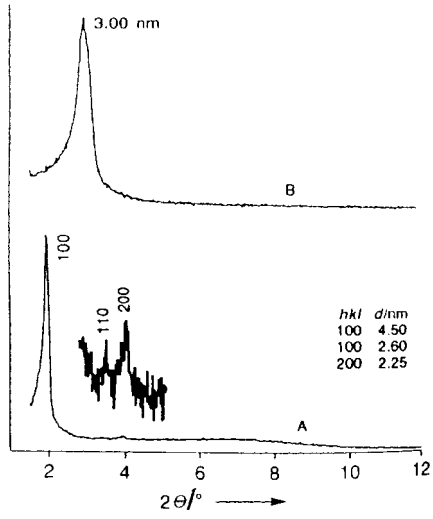

Figure 38. X-ray diffraction pattern of the zirconium oxide compound synthesized with zirconium propoxide as the Zr source. As synthesized (A); after calcination (B) [235]. Reprinted with permission from *Ang. Chem. int. Ed. Engl.*, 1996, **35**, 541.

A particularly exciting development for this synthetic process was the synthesis of mesoporous platinum metal films by electrochemical reduction of platinum salts confined in the aqueous regions of lyotropic liquid crystal phases [241]. The deposited platinum films were of uniform thickness, were very flat, and had regular mesoporous structure and high specific surface areas. The pore diameter was varied by using POE surfactant templates of different chain length, and by the use of *n*-heptane as an auxiliary swelling agent. Geometric deposition of the channels was determined by the architecture of the liquid crystal phase. Cyclic voltammetry measurements showed that the films possessed good electrical connectivity and allowed fast electrolyte diffusion; it was suggested that they could perform well as electrochemical capacitors at high power and high frequency. The films also had good mechanical and electrochemical stability. Such platinum materials have interesting applications as mesoporous electrodes for batteries, fuel cells, electrochemical capacitors, and sensors.

12.3. *Further applications*

Advanced separation/purification, electronic, optical and electron transfer applications have been suggested for MCM-41-type materials, generally relying on the special characteristics of species encapsulated in the material mesopores. Some of the potential applications other than in catalysis are outlined below.

12.3.1. *Stationary phases for chromatography*

The properties of aluminosilicate MCM-41 in normal phase high-performance liquid chromatography (HPLC) was investigated by Grun *et al.* [242]. It was reported that the mesoporous stationary phase, which had pore diameters of 4 nm, had acidic and basic properties making it suitable for chromatographic separations of acidic, neutral and basic compounds.

12.3.2. *Environmental remediation*

Mercier and Pinnavaia produced MCM-41 containing a high density of thiol groups grafted to the mesopore surfaces [243]. The material was reported to have selective absorptive properties for mercury and lead. The

‡Octaethylene glycol monohexadecyl ether.

surface derivatization may therefore be a route for the production of heavy metal adsorbents for the cleansing of toxic environments.

12.3.3. *Mini-reactors for electron transfer reactions*

2,4,6-Triphenylpyrilium (TP^+) has been found to be a highly efficient electron transfer agent when incorporated into MCM-41 [244]. In the presence of long wavelength radiation, the MCM-41-confined TP^+ can be used as a sensitizer to convert *cis*-stilbene to *trans*-stilbene. In MCM-41, the TP^+ was much more effective at this conversion than $TP^+BF_4^-$, TP^+ incorporated into Y zeolite, or TP^+ on amorphous silica/alumina. This behaviour suggests that mesoporous hosts are promising for making nanoscopic products in a uniform way (by photoinduced electron transfer reactions), which has not been possible with any other material.

12.3.4. *Mesoporous hosts for quantum confinement*

Fe_2O_3 nanoparticles were made within the pores of a mesoporous silicate by Abe *et al.* and it was observed that the usual band gap of 2.1 eV had risen to 4.1 eV for the nanoparticles [245]. It was suggested that this rise was due to the *quantum-size effect*. SiGe quantum dots were prepared within an ordered mesoporous substrate by Tang *et al.* [246]. Improved luminescence characteristics were reported for these species, and optoelectronic applications for the materials were suggested. Quantum-size effects were also reported for buckminsterfullerine, C_{60}, immobilized within MCM-41 [247, 248].

12.3.5. *Mesoporous supports for molecular wires*

Conducting polyaniline and carbon filaments have been synthesized within the pore system of aluminosilicate MCM-41 materials [249–253], see figure 39. In order to produce the polyaniline fibres, aniline vapour was first adsorbed, and then reacted with peroxydisulfate to form polymers several hundred aniline rings in length. Carbon filaments were formed by first introducing acrylonitrile monomers via vapour or solution transfer into the mesoporous host, and allowing them to polymerize in the channels with external radical initiators. Pyrolysis of the intra-channel polyacrylonitrile resulted in filaments whose microwave conductivity is about 10 times that of bulk carbonized polyacrylonitrile.

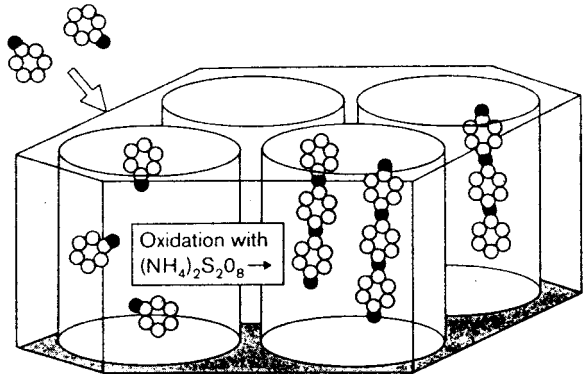

Figure 39. Schematic representation of the encapsulation of polyaniline in MCM-41 channels.

Molecular or quantum wires have applications in various hi-technology electronic devices and both of the above results provide a considerable step forward in the design of nanometer-scale electronic devices. Additionally, the inclusion of organic polymers in the mesopores of MCM-41-type silica can lead to materials with interesting mechanical properties.

12.3.6. *Shape-selective polymerization*

The controlled polymerizations of styrene, methyl methacrylate and vinyl acetate were carried out in MCM-41 materials with pore sizes of 2.5 and 4 nm [254]. The hosts with smaller holes produce longer polymer chains. The authors explained this phenomenon by suggesting that there are fewer growing chains which can interact with the monomers in solution. The glass transition for the polyvinyl acetate polymers was 20 K lower for the confined polymer (2.5 nm pores) than for the 'free' product. This observation can be attributed to the suppression of co-operative motion of the polymers.

It has been suggested that liquid crystal templating concepts could be applied to protein synthesis [255]. Protein inclusion in porous silicate lattices can occur, provided that the dimensions of the pores and the particular protein are appropriately chosen (see figure 40). The highly ordered tubes would be expected to provide a sequencing influence on the protein molecules. Bicontinuous cubic phases consisting of surfactant alone may be sufficiently rigid to order the protein molecules into a regular lattice.

It is worth noting that detergents (i.e. surfactants) are routinely used to crystallize membrane proteins. The role of the amphiphiles is poorly understood, but it is proposed in this paper that they promote crystallization via the intrinsic self-assembly properties of the protein–surfactant mixture.

13. Conclusion

In this review we have aimed to cover most aspects of the synthesis, characterization and to some extent the applications of regular porous inorganic structures templated by liquid crystal templating routes. As can be seen from the plot at the beginning of the review of papers published in this field since the discovery of MCM-41 in 1992, scientific interest in the field of LCT is still booming. Certain mesoporous materials are now tuneable to desired applications and we foresee that

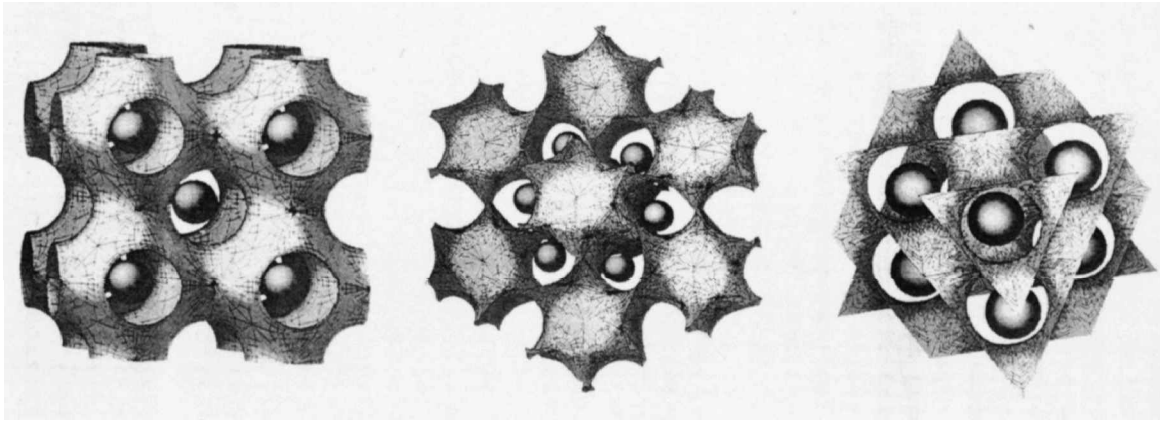

(*a*) (*b*) (*c*)

Figure 40. Cubic structures found in liquid crystal systems. Spheres indicate tentative protein positions: (*a*) P-surface, space group *Im*3*m*; (*b*) gyroid, space group *Ia*3*d*; (*c*) D-surface, space group *Pn*3*m* [255]. Reprinted with permission from *Acta chemica Scan*., 1994, **48,** 88.

such materials will become available commercially for advanced industrial applications in the near future.

References

[1] Beck, J. S., Vartuli, J. C., Roth, W. J., Leonowicz, M. E., Kresge, C. T., Schmitt, K. D., Chu, C. T. W., Olson, D. H., Sheppard, E. W., McCullen, S. B., Higgins, J. B., and Schlenker, J. L., 1992, *J. Am. chem. Soc*., **114,** 10 834.

[2] Kresge, C. T., Leonowicz, M. E., Roth, W. J., Vartuli, J. C., and Beck, J. S., 1992, *Nature*, **359,** 710.

[3] Maschmeyer, T., 1998, *Curr. Opin. solid State mater. Sci*., **3,** 71.

[4] Beck, J. S., and Vartuli, J. C., 1996, *Curr. Opin. solid State mater. Sci*., **1,** 76.

[5] Antonelli, D. M., and Ying, J. Y., 1996, *Curr. Opin. Colloid Interface Sci*., **1,** 523.

[6] Sayari, A., 1996, *Stud. surf. Sci. Catal*., **102,** 1.

[7] Sayari, A., and Liu, P., 1997, *Microporous Mater*., **12,** 149.

[8] Stucky, G. D., Huo, Q. S., Firouzi, A., Chmelka, B. F., Schacht, S., VoigtMartin, I. G., and Schuth, F., 1997, *Stud. surf. Sci. Catal*., **105,** 3.

[9] Corma, A., 1997, *Chem. Rev*., **97,** 2373.

[10] Corma, A., 1997, *Top. Catal*., **4,** 249.

[11] Göltner, C. G., and Antonietti, M., 1997, *Adv. Mater*., **9,** 431.

[12] Ozin, G. A., Chomski, E., Khushalani, D., and MacLachlan, M. J., 1998, *Curr. Opin. Colloid Interface Sci*., **3,** 181.

[13] Zhao, D. Y., Yang, P. D., Huo, Q. S., Chmelka, B. F., and Stucky, G. D., 1998, *Curr. Opin. solid State mater. Sci*., **3,** 111.

[14] Schuth, F., 1998, *Curr. Opin. Colloid Interface Sci*., **3,** 174.

[15] Mann, S., Burkett, S. L., Davis, S. A., Fowler, C. E., Mendelson, N. H., Sims, S. D., Walsh, D., and Whilton, N. T., 1997, *Chem. Mater*., **9,** 2300.

[16] Brinker, C. J., 1998, *Curr. Opin. Colloid Interface Sci*., **3,** 166.

[17] Lok, B. M., Cannan, T. R., and Messina, C. A., 1983, *Zeolites*, **3,** 282.

[18] Lewis, D. W., Catlow, C. R. A., and Thomas, J. M., 1996, *Chem. Mater*., **8,** 1112.

[19] Lewis, D. W., Willock, D. J., Catlow, C. R. A., Thomas, J. M., and Hutchings, G. J., 1996, *Nature*, **382,** 604.

[20] Lewis, D. W., and Willock, D. J., 1996, *Abs. Am. chem. Soc*., **212,** 123.

[21] Lewis, D. W., Bell, R. G., Wright, P. A., Catlow, C. R. A., and Thomas, J. M., 1997, *Stud. surf. Sci. Catal*., **105,** 2291.

[22] Lewis, D. W., Sankar, G., Wyles, J. K., Thomas, J. M., Catlow, C. R. A., and Willock, D. J., 1997, *Ang. Chem. int. Ed. Engl*., **36,** 2675.

[23] Lewis, D. W., Catlow, C. R. A., and Thomas, J. M., 1997, *J. chem. Soc., Faraday Discuss*., 451.

[24] Seddon, J. M., and Templer, R. H., 1993, *Phil. Trans. roy. Soc. Lond. A*, **344,** 377.

[25] Bissell, R., and Boden, N., 1995, *Chemistry in Britain*, **31,** 38.

[26] Warnheim, T., and Jonsson, A., 1988, *J. Coll. and Interface Sci*., **125,** 627.

[27] Kresge, C. T., Vartuli, J. C., Roth, W. J., Leonowicz, M. E., Beck, J. S., Schmitt, K. D., Chu, C. T. W., Olson, D. H., Sheppard, E. W., McCullen, S. B., Higgins, J. B., and Schlenker, J. L., 1995, *Stud. surf. Sci. Catal*., **92,** 11.

[28] Beck, J. S., Vartuli, J. C., Kennedy, G. J., Kresge, C. T., Roth, W. J., and Schramm, S. E., 1994, *Chem. Mater*., **6,** 1816.

[29] Huo, Q. S., Margolese, D. I., Ciesla, U., Feng, P. Y., Gier, T. E., Sieger, P., Leon, R., Petroff, P. M., Schuth, F., and Stucky, G. D., 1994, *Nature*, **368,** 317.

[30] Vartuli, J. C., Schmitt, K. D., Kresge, C. T., Roth, W. J., Leonowicz, M. E., McCullen, S. B., Hellring, S. D., Beck, J. S., Schlenker, J. L., Olson, D. H., and Sheppard, E. W., 1994, *Chem. Mater*., **6,** 2317.

[31] Vartuli, J. C., Kresge, C. T., Roth, W. J., Schmitt, K. D., McCullen, S. B., Beck, J. S., Leonowicz, M. E., Lutner, J. D., and Sheppard, E. W., 1995, *Abs. Am. chem. Soc*., **209,** 27.
[32] Edler, K. J., Dougherty, J., Durand, R., Iton, L., Kirton, G., Lockhart, G., Wang, Z., Withers, R., and White, J. W., 1995, *Colloids and Surfaces A*, **102,** 213.
[33] Edler, K. J., and White, J. W., 1997, *Chem. Mater*., **9,** 1226.
[34] Brown, A. S., Edler, K. J., Gentle, I., Kirton, G. E., Reynolds, P. A., Saville, P. W., Watson, J., and White, J. W., 1997, The Rutherford Appleton Laboratory ISIS facility Annual Report 1996–1997, p. 52.
[35] Edler, K. J., Reynolds, P. A., White, J. W., and Cookson, D., 1997, *J. chem. Soc., Faraday Trans*., **93,** 199.
[36] Ravikovitch, P. I., Wie, D., Chueh, W. T., Haller, G. L., and Neimark, A. V., 1997, *J. phys. Chem. B*, **101,** 3671.
[37] Edler, K. J., Reynolds, P. A., and White, J. W., 1998, *J. phys. Chem. B*, **102,** 3676.
[38] Schmidt, R., Stocker, M., Akporiaye, D., Torstad, E. H., and Olsen, A., 1995, *Microporous Mater*., **5,** 1.
[39] Vartuli, J. C., Schmitt, K. D., Kresge, C. T., Roth, W. J., Leonowicz, M. E., McCullen, S. B., Hellring, S. D., Beck, J. S., Schlenker, J. L., Olson, D. H., and Sheppard, E. W., 1994, *Stud. surf. Sci. Catal*., **84,** 53.
[40] Alfredsson, V., and Anderson, M. W., 1996, *Chem. Mater*., **8,** 1141.
[41] Alfredsson, V., Anderson, M. W., Ohsuna, T., Terasaki, O., Jacob, M., and Bojrup, M., 1997, *Chem. Mater*., **9,** 2066.
[42] Kim, J. M., Kim, S. K., and Ryoo, R., 1998, *J. chem. Soc., chem. Commun*., 259.
[43] Ko, C. H., and Ryoo, R., 1996, *J. chem. Soc., chem. Commun*., 2467.
[44] Ryoo, R., Kim, J. M., Ko, C. H., and Shin, C. H., 1996, *J. phys. Chem*., **100,** 17 718.
[45] Monnier, A., Schuth, F., Huo, Q., Kumar, D., Margolese, D., Maxwell, R. S., Stucky, G. D., Krishnamurty, M., Petroff, P., Firouzi, A., Janicke, M., and Chmelka, B. F., 1993, *Science*, **261,** 1299.
[46] Luan, Z. H., He, H. Y., Zhou, W. Z., and Klinowski, J., 1998, *J. chem. Soc., Faraday Trans*., **94,** 979.
[47] Alfredsson, V., Keung, M., Monnier, A., Stucky, G. D., Unger, K. K., and Schuth, F., 1994, *J. chem. Soc., chem. Commun*., 921.
[48] Steel, A., Carr, S. W., and Anderson, M. W., 1994, *J. chem. Soc., chem. Commun*., 1571.
[49] Steel, A., Carr, S. W., and Anderson, M. W., 1995, *Chem. Mater*., **7,** 1829.
[50] Chen, C. Y., Xiao, S. Q., and Davis, M. E., 1993, *Microporous Mater*., **2,** 27.
[51] Stucky, G. D., Monnier, A., Schuth, F., Huo, Q., Margolese, D., Kumar, D., Krishnamurty, M., Petroff, P., Firouzi, A., Janicke, M., and Chmelka, B. F., 1994, *Mol. Cryst. liq. Cryst*., **240,** 187.
[52] Ciesla, U., Demuth, D., Leon, R., Petroff, P., Stucky, G., Unger, K., and Schuth, F., 1994, *J. chem. Soc., chem. Commun*., 1387.
[53] Bull, L. M., Kumar, D., Millar, S. P., Besier, T., Janicke, M., Stucky, G. D., and Chmelka, B. F., 1994, *Stud. surf. Sci. Catal*., **84,** 429.
[54] Firouzi, A., Kumar, D., Bull, L. M., Besier, T., Sieger, P., Hue, Q., Walker, S. A., Zasadzinski, J. A., Glinka, C., Nicol, J., Margolese, D., Stucky, G. D., and Chmelka, B. F., 1995, *Science*, **267,** 1138.
[55] Huo, Q., Leon, R., Petroff, P. M., and Stucky, G. D., 1995, *Science*, **268,** 1324.
[56] Glinka, C. J., Nicol, J. M., Stucky, G. D., Ramli, E., Margolese, D. I., and Huo, Q., 1995, in *Advances in Porous Materials; Mater. Res. Proc*., Vol. 341, edited by S. Komarneni, D. M. Smith, and J. S. Beck, Materials Research Society, Pittsburgh, PA, p. 47.
[57] Calabro, D. C., Valyocsik, E. W., and Ryan, F. X., 1996, *Microporous Mater*., **7,** 243.
[58] Cheng, C. F., Luan, Z. H., and Klinowski, J., 1995, *Langmuir*, **11,** 2815.
[59] Cheng, C. F., He, H. Y., Zhou, W. Z., and Klinowski, J., 1995, *Chem. Phys. Lett*., **244,** 117.
[60] Huo, Q. S., Margolese, D. I., Ciesla, U., Demuth, D. G., Feng, P. Y., Gier, T. E., Sieger, P., Firouzi, A., Chmelka, B. F., Schuth, F., and Stucky, G. D., 1994, *Chem. Mater*., **6,** 1176.
[61] Regev, O., 1996, *Langmuir*, **12,** 4940.
[62] Firouzi, A., Atef, F., Oertli, A. G., Stucky, G. D., and Chmelka, B. F., 1997, *J. Am. chem. Soc*., **119,** 3596.
[63] Israelachvili, J. N., 1991, *Intermolecular and Surface Forces* (London: Academic Press).
[64] Linden, M., Schunk, S. A., and Schuth, F., 1998, *Ang. Chem. int. Ed. Engl*., **37,** 821.
[65] Galarneau, A., DiRenzo, F., Fajula, F., Mollo, L., Fubini, B., and Ottaviani, M. F., 1998, *J. Colloid Interface Sci*., **201,** 105.
[66] Huo, Q. S., Margolese, D. I., and Stucky, G. D., 1996, *Chem. Mater*., **8,** 1147.
[67] Khushalani, D., Kuperman, A., Coombs, N., and Ozin, G. A., 1996, *Chem. Mater*., **8,** 2188.
[68] Behrens, P., 1996, *Ang. Chem. int. Ed. Engl*., **35,** 515.
[69] Kloetstra, K. R., Jansen, J. C., Zandbergen, H. W., and VanBekkum, H., 1997, *Abs. Am. chem. Soc*., **214,** 14.
[70] Kloetstra, K. R., VanBekkum, H., and Jansen, J. C., 1997, *J. chem. Soc., chem. Commun*., 2281.
[71] Kim, J. M., and Ryoo, R., 1996, *Bull. Korean chem. Soc*., **17,** 66.
[72] Ryoo, R., and Jun, S., 1997, *J. phys. Chem. B*, **101,** 317.
[73] Behrens, P., Glaue, A., Haggenmuller, C., and Schechner, G., 1997, *Solid State Ionics*, **101,** 255.
[74] Coustel, N., Direnzo, F., and Fajula, F., 1994, *J. chem. Soc., chem. Commun*., 967.
[75] DiRenzo, F., Coustel, N., Mendiboure, M., Cambon, H., and Fajula, F., 1997, *Stud. surf. Sci. Catal*., **105,** 69.
[76] Kruk, M., Jaroniec, M., Ryoo, R., and Kim, J. M., 1997, *Microporous Mater*., **12,** 93.
[77] Ryoo, R., and Kim, J. M., 1995, *J. chem. Soc., chem. Commun*., 711.
[78] Ryoo, R., Kim, J. M., Shin, C. H., and Lee, L. Y., 1997, *Stud. surf. Sci. Catal*., **105,** 45.
[79] Edler, K. J., and White, J. W., 1995, *J. chem. Soc., chem. Commun*., 155.

[80] Cheng, C. F., Park, D. H., and Klinowski, J., 1997, *J. chem. Soc., Faraday Trans.*, **93,** 193.
[81] Ulagappan, N., and Rao, C. N. R., 1996, *J. chem. Soc., chem. Commun.*, 2759.
[82] Khushalani, D., Kuperman, A., Ozin, G. A., Tanaka, K., Garces, J., and Olken, M. M., 1996, *Adv. Mater.*, **7,** 842.
[83] Cheng, C. F., Zhou, W. Z., Park, D. H., Klinowski, J., Hargreaves, M., and Gladden, L. F., 1997, *J. chem. Soc., Faraday Trans.*, **93,** 359.
[84] Sayari, A., Liu, P., Kruk, M., and Jaroniec, M., 1997, *Chem. Mater.*, **9,** 2499.
[85] Sayari, A., Kruk, M., and Jaroniec, M., 1997, *Catal. Lett.*, **49,** 147.
[86] Lohse, U., Bertram, R., Jancke, K., Kurzawski, I., Parlitz, B., Loffler, E., and Schreier, E., 1995, *J. chem. Soc., Faraday Trans.*, **91,** 1163.
[87] Girnus, I., Jancke, K., Vetter, R., Richtermendau, J., and Caro, J., 1995, *Zeolites*, **15,** 33.
[88] Arafat, A., Jansen, J. C., Ebaid, A. R., and Vanbekkum, H., 1993, *Zeolites*, **13,** 162.
[89] Wu, C. G., and Bein, T., 1996, *J. chem. Soc., chem. Commun.*, 925.
[90] Borade, R. B., and Clearfield, A., 1995, *Catal. Lett.*, **31,** 267.
[91] Janicke, M., Kumar, D., Stucky, G. D., and Chmelka, B. F., 1994, *Stud. surf. Sci. Catal.*, **84,** 243.
[92] Kloetstra, K. R., Zandbergen, H. W., and Vanbekkum, H., 1995, *Catal. Lett.*, **33,** 157.
[93] Luan, Z. H., Cheng, C. F., Zhou, W. Z., and Klinowski, J., 1995, *J. phys. Chem.*, **99,** 1018.
[94] Luan, Z. H., He, H. Y., Zhou, W. Z., Cheng, C. F., and Klinowski, J., 1995, *J. chem. Soc., Faraday Trans.*, **91,** 2955.
[95] Ryoo, R., Ko, C. H., and Howe, R. F., 1997, *Chem. Mater.*, **9,** 1607.
[96] Schmidt, R., Akporiaye, D., Stocker, M., and Ellestad, O. H., 1994, *J. chem. Soc., chem. Commun.*, 1493.
[97] Schmidt, R., Akporiaye, D., Stocker, M., and Ellestad, O. H., 1994, *Stud. surf. Sci. Catal.*, **84,** 61.
[98] Hamdan, H., Endud, S., He, H. Y., Muhid, M. N. M., and Klinowski, J., 1996, *J. chem. Soc., Faraday Trans.*, **92,** 2311.
[99] Romero, A. A., Alba, M. D., Zhou, W. Z., and Klinowski, J., 1997, *J. phys. Chem. B*, **101,** 5294.
[100] Romero, A. A., Alba, M. D., and Klinowski, J., 1998, *J. phys. Chem. B*, **102,** 123.
[101] Tanev, P. T., and Pinnavaia, T. J., 1995, *Science*, **267,** 865.
[102] Bagshaw, S. A., Prouzet, E., and Pinnavaia, T. J., 1995, *Science*, **269,** 1242.
[103] Tanev, P. T., and Pinnavaia, T. J., 1996, *Chem. Mater.*, **8,** 2068.
[104] Zhang, W. Z., Pauly, T. R., and Pinnavaia, T. J., 1997, *Chem. Mater.*, **9,** 2491.
[105] Prouzet, E., and Pinnavaia, T. J., 1997, *Ang. Chem. int. Ed. Engl.*, **36,** 516.
[106] Brinker, C. J., 1988, *J. non-cryst. Solids*, **100,** 31.
[107] Karra, V. R., and Sayari, A., 1995, *Abs. Am. chem. Soc.*, **209,** 9.
[108] Sayari, A., Danumah, C., and Moudrakovski, I. L., 1995, *Chem. Mater.*, **7,** 813.
[109] Huo, Q. S., Sieger, P., Firouzi, A., Chmelka, B. F., and Stucky, G. D., 1995, *Abs. Am. chem. Soc.*, **209,** 283.
[110] Velev, O. D., Jede, T. A., Lobo, R. F., and Lenhof, A. M., 1997, *Nature*, **389,** 447.
[111] Imhof, A., and Pine, D. J., 1997, *Nature*, **389,** 948.
[112] Zhao, D. Y., Feng, J. L., Huo, Q. S., Melosh, N., Fredrickson, G. H., Chmelka, B. F., and Stucky, G. D., 1998, *Science*, **279,** 548.
[113] Templin, M., Frank, A., DuChesne, A., Leist, H., Zhang, Y., Ulrich, R., Schädler, V., and Wiesner, U., 1997, *Science*, **278,** 1795.
[114] Inagaki, S., Fukushima, Y., and Kuroda, K., 1993, *J. chem. Soc., chem. Commun.*, 680.
[115] Inagaki, S., Fukushima, Y., and Kuroda, K., 1994, *Stud. surf. Sci. Catal.*, **84,** 125.
[116] Inagaki, S., Yamada, Y., Fukushima, Y., and Kuroda, K., 1995, *Stud. surf. Sci. Catal.*, **92,** 143.
[117] Inagaki, S., Koiwai, A., Suzuki, N., Fukushima, Y., and Kuroda, K., 1996, *Bull. chem. Soc. Jpn.*, **69,** 1449.
[118] Vartuli, J. C., Kresge, C. T., Leonowicz, M. E., Chu, C. T.-W., McCullen, S. B., Beck, J. S., Johnson, I. D., and Sheppard, E. W., 1994, *Chem. Mater.*, **6,** 2070.
[119] Chen, C. Y., Xiao, S. Q., and Davis, M. E., 1995, *Microporous Mater.*, **4,** 1.
[120] Inagaki, S., Sakamoto, Y., Fukushima, Y., and Terasaki, O., 1996, *Chem. Mater.*, **8,** 2089.
[121] Inagaki, S., Fukushima, Y., Kuroda, K., and Kuroda, K., 1996, *J. Colloid Interface Sci.*, **180,** 623.
[122] Branton, P. J., Kaneko, K., Setoyama, N., Sing, K. S. W., Inagaki, S., and Fukushima, Y., 1996, *Langmuir*, **12,** 599.
[123] Inagaki, S., Yamada, Y., and Fukushima, Y., 1997, *Stud. surf. Sci. Catal.*, **105,** 109.
[124] Attard, G. S., Glyde, J. C., and Göltner, C. G., 1995, *Nature*, **378,** 366.
[125] Attard, G. S., Edgar, M., and Göltner, C. G., 1998, *Acta Mater.*, **46,** 751.
[126] Mitchell, D. J., Tiddy, G. J. T., Waring, L., Bostock, T., and McDonald, M. P., 1983, *J. chem. Soc., Faraday Trans. 1.*, **79,** 975.
[127] Weissenberger, M. C., Göltner, C. G., and Antonietti, M., 1997, *Ber. Bunsenges. Phys.*, **101,** 1679.
[128] Gray, D. H., Hu, S., Juang, E., and Gin, D. L., 1997, *Adv. Mater.*, **9,** 731.
[129] McGrath, K. M., Dabbs, D. M., Yao, N., Aksay, I. A., and Gruner, S. M., 1997, *Science*, **277,** 552.
[130] Frisch, H. L., West, J. M., Göltner, C. G., and Attard, G. S., 1996, *J. Polym. Sci. A, Polym. Chem.*, **34,** 1823.
[131] Huo, Q. S., Feng, J. L., Schuth, F., and Stucky, G. D., 1997, *Chem. Mater.*, **9,** 14.
[132] Firouzi, A., Schaefer, D. J., Tolbert, S. H., Stucky, G. D., and Chmelka, B. F., 1997, *J. Am. chem. Soc.*, **119,** 9466.
[133] Yang, H., Coombs, N., and Ozin, G. A., 1997, *Nature*, **386,** 692.
[134] Ryoo, R., Ko, C. H., Cho, S. J., and Kim, J. M., 1997, *J. phys. Chem. B*, **101,** 10 610.
[135] Anderson, M. T., Martin, J. E., Odinek, J. G., Newcomer, P. P., and Wilcoxon, J. P., 1997, *Microporous Mater.*, **10,** 13.
[136] Martin, J. E., Anderson, M. T., Odinek, J. O., and Newcomer, P., 1997, *Langmuir*, **13,** 4133.
[137] Ogawa, M., 1994, *J. Am. chem. Soc.*, **116,** 7941.
[138] Ogawa, M., 1996, *J. chem. Soc., chem. Commun.*, 1149.

[139] Ogawa, M., and Igarashi, T., Kuroda, K., 1997, *Bull. chem. Soc. Jpn.*, **70,** 2833.
[140] Ogawa, M., and Kuroda, K., 1997, *Bull. chem. Soc. Jpn.*, **70,** 2593.
[141] Lu, Y., Gangli, R., Drewien, D. M., Anderson, M. T., Brinker, C. J., Gong, W., Guo, Y., Soyez, H., Dunn, B., Huang, M. H., and Zink, J. I., 1997, *Nature*, **389,** 364.
[142] Bruisma, P. J., Kim, A. Y., Liu, J., and Baskaran, S., 1997, *Chem. Mater.*, **9,** 2507.
[143] Grun, M., Lauer, I., and Unger, K. K., 1997, *Adv. Mater.*, **9,** 254.
[144] Yang, H., Vovk, G., Coombs, N., Sokolov, I., and Ozin, G. A., 1998, *J. mater. Chem.*, **8,** 743.
[145] Yang, H., Kuperman, A., Coombs, N., Mamicheafara, S., and Ozin, G. A., 1996, *Nature*, **379,** 703.
[146] Yang, H., Coombs, N., Sokolov, I., and Ozin, G. A., 1996, *Nature*, **381,** 589.
[147] Yang, H., Coombs, N., Sokolov, I., and Ozin, G. A., 1997, *J. mater. Chem.*, **7,** 1285.
[148] Aksay, I. A., Trau, M., Manne, S., Honma, I., Yao, N., Zhou, L., Fenter, P., Eisenberger, P. M., and Gruner, S. M., 1996, *Science*, **273,** 892.
[149] Manne, S., Cleveland, J. P., Gaub, H. E., Stucky, G. D., and Hansma, P. K., 1994, *Langmuir*, **10,** 4409.
[150] Manne, S., Schaffer, T. E., Huo, Q., Hansma, P. K., Morse, D. E., Stucky, G. D., and Aksay, I. A., 1997, *Langmuir*, **13,** 6382.
[151] Yang, H., Coombs, N., Dag, O., Sokolov, I., and Ozin, G. A., 1997, *J. mater. Chem.*, **7,** 1755.
[152] Brown, A. S., Holt, S. A., Dam, T., Trau, M., and White, J. W., 1997, *Langmuir*, **13,** 6363.
[153] Yang, H., Coombs, N., and Ozin, G. A., 1998, *J. mater. Chem.*, **8,** 1205.
[154] Schacht, S., Huo, Q., Voigtmartin, I. G., Stucky, G. D., and Schuth, F., 1996, *Science*, **273,** 768.
[155] Huo, Q. S., Zhao, D. Y., Feng, J. L., Weston, K., Buratto, S. K., Stucky, G. D., Schacht, S., and Schuth, F., 1997, *Adv. Mater.*, **9,** 974.
[156] Tolbert, S. H., Schaffer, T. E., Feng, J. L., Hansma, P. K., and Stucky, G. D., 1997, *Chem. Mater.*, **9,** 1962.
[157] Shariff, S. B., 1998, Undergraduate research project report, Department of Chemistry, Imperial College, London.
[158] Yang, H., Coombs, N., and Ozin, G. A., 1997, *Adv. Mater.*, **9,** 811.
[159] Edler, K. J., Reynolds, P. A., Brown, A. S., Slawecki, T. M., and White, J. W., 1998, *J. chem. Soc., Faraday Trans.,* **94,** 1287.
[160] Hillhouse, H. W., Okubo, T., Van Egmond, J. W., and Tsapatsis, M., 1997, *Chem. Mater.*, **9,** 1505.
[161] Trau, M., Yao, N., Kim, E., Xia, Y., Whitesides, G. M., and Aksay, I. A., 1997, *Nature*, **390,** 674.
[162] Tolbert, S. H., Firouzi, A., Stucky, G. D., and Chmelka, B. F., 1997, *Science*, **278,** 264.
[163] Raimondi, M. E., Maschmeyer, T., Templer, R. H., and Seddon, J. M., 1997, *J. chem. Soc., chem. Commun.,* 1843.
[164] Leadbeater, B. S. C., and Riding, R. (editors), 1986, *Biomineralisation in Lower Plants and Animals* (Oxford: Clarendon Press).
[165] Mann, S., and Ozin, G. A., 1996, *Nature*, **382,** 313.
[166] Ball, P., 1995, *New Scientist*, **148,** 42.
[167] Oliver, S., Kuperman, A., Coombs, N., Lough, A., and Ozin, G. A., 1995, *Nature*, **378,** 47.
[168] Oliver, S., Coombs, N., and Ozin, G. A., 1995, *Adv. Mater.*, **7,** 931.
[169] Ozin, G. A., and Oliver, S., 1995, *Adv. Mater.*, **7,** 943.
[170] Ozin, G. A., 1997, *Acc. chem. Res.*, **30,** 17.
[171] Ozin, G. A., Yang, H., Sokolov, I., and Coombs, N., 1997, *Adv. Mater.*, **9,** 662.
[172] Ozin, G. A., Varaksa, N., Coombs, N., Davies, J. E., Perovic, D. D., and Ziliox, M., 1997, *J. mater. Chem.*, **7,** 1601.
[173] Belcher, A. M., Hansma, P. K., Stucky, G. D., and Morse, D. E., 1998, *Acta Mater.*, **46,** 733.
[174] Oliver, S. R. J., and Ozin, G. A., 1998, *J. mater. Chem.*, **8,** 1081.
[175] Walsh, D., and Mann, S., 1995, *Nature*, **377,** 320.
[176] Zaremba, C. M., and Stucky, G. D., 1996, *Curr. Opin. Solid State Mater. Sci.*, **1,** 425.
[177] Tanev, P. T., and Pinnavaia, T. J., 1996, *Science*, **271,** 1267.
[178] Tanev, P. T., Liang, Y., and Pinnavaia, T. J., 1997, *J. Am. chem. Soc.*, **119,** 8616.
[179] Lim, H.-P., and Mou, C.-Y., 1996, *Science*, **273,** 765.
[180] Archibald, D. D., and Mann, S., 1993, *Nature*, **364,** 430.
[181] Davis, S. A., Burkett, S. L., Mendelson, N. H., and Mann, S., 1997, *Nature*, **385,** 420.
[182] Llewellyn, P. L., Schuth, F., Grillet, Y., Rouquerol, F., Rouquerol, J., and Unger, K. K., 1995, *Langmuir*, **11,** 574.
[183] Schmidt, R., Stocker, M., Hansen, E., Akporiaye, D., and Ellestad, O. H., 1995, *Microporous Mater.*, **3,** 443.
[184] Akporiaye, D., Hansen, E. W., Schmidt, R., and Stocker, M., 1994, *J. phys. Chem.*, **98,** 1926.
[185] Franke, O., Schulzekloff, G., Rathousky, J., Starek, J., and Zukal, A., 1993, *J. chem. Soc., chem. Commun.*, 724.
[186] Branton, P. J., Hall, P. G., and Sing, K. S. W., 1993, *J. chem. Soc., chem. Commun.*, 1257.
[187] Branton, P. J., Hall, P. G., Sing, K. S. W., Reichert, H., Schuth, F., and Unger, K. K., 1994, *J. chem. Soc., Faraday Trans.,* **90,** 2965.
[188] Branton, P. J., Hall, P. G., Treguer, M., and Sing, K. S. W., 1995, *J. chem. Soc., Faraday Trans.*, **91,** 2041.
[189] Branton, P. J., Hall, P. G., and Sing, K. S. W., 1995, *J. Int. Adsorption Soc.*, **1,** 77.
[190] Branton, P. J., Sing, K. S. W., and White, J. W., 1997, *J. chem. Soc., Faraday Trans.,* **93,** 2337.
[191] Corma, A., Navarro, M. T., and Pariente, J. P., 1994, *J. chem. Soc., chem. Commun.,* 147.
[192] Corma, A., Navarro, M. T., Perezpariente, J., and Sanchez, F., 1994, *Stud. surf. Sci. Catal.*, **84,** 69.
[193] Tanev, P. T., Chibwe, M., and Pinnavaia, T. J., 1994, *Nature*, **368,** 321.
[194] Franke, O., Rathousky, J., Schulzekloff, G., Starek, J., and Zukal, A., 1994, *Stud. surf. Sci. Catal.*, **84,** 77.
[195] Maschmeyer, T., Rey, F., Sankar, G., and Thomas, J. M., 1995, *Nature*, **378,** 159.
[196] Corma, A., Martinez, A., and Martinez-Soria, V., 1997, *J. Catal.*, **169,** 4880.

[197] Junges, U., Jacobs, W., Voigtmartin, I., Krutzsch, B., and Schuth, F., 1995, *J. chem. Soc., chem. Commun.*, 2283.

[198] Junges, U., Schuth, F., Schmid, G., Uchida, Y., and Schlogl, R., 1997, *Ber. Bunsenges. Phys.*, **101,** 1631.

[199] Reddy, K. M., Moudrakovski, I., and Sayari, A., 1994, *J. chem. Soc., chem. Commun.,* 1059.

[200] Morey, M., Davidson, A., Eckert, H., and Stucky, G. D., 1997, *Chem. Mater.*, **8,** 486.

[201] Luan, Z. H., Xu, J., He, H. Y., Klinowski, J., and Kevan, L., 1996, *J. phys. Chem.*, **100,** 19 595.

[202] Zhao, D. Y., and Goldfarb, D., 1995, *J. chem. Soc., chem. Commun.*, 875.

[203] Sutra, P., and Brunel, D., 1996, *J. chem. Soc., chem. Comm.*, 2485.

[204] Kim, S. S., Zhang, W. Z., and Pinnavaia, T. J., 1997, *Catal. Lett.*, **43,** 149.

[205] On, D. T., Joshi, P. N., and Kaliaguine, S., 1996, *J. phys. Chem.*, **100,** 6743.

[206] Sayari, A., Moudrakovski, I., Danumah, C., Ratcliffe, C. I., Ripmeester, J. A., and Preston, K. F., 1995, *J. phys. Chem.*, **99,** 16 373.

[207] Tuel, A., and Gontier, S., 1996, *Chem. Mater.*, **8,** 114.

[208] Armengol, E., Cano, M. L., Corma, A., Garcia, H., and Navarro, M. T., 1995, *J. chem. Soc., chem. Commun.,* 519.

[209] Clark, J. H., Ross, J. V., Macquarrie, D. J., Barlow, S. J., and Bastock, T., 1997, *J. chem. Soc., chem. Commun.*, **13,** 1203.

[210] Ko, Y. S., Han, T. K., Park, J. W., and Woo, S. I., 1996, *Macromol. Rapid Commun.*, **17,** 749.

[211] Kloetstra, K. R., vanLaren, M., and VanBekkum, H., 1997, *J. chem. Soc., Faraday Trans.*, **93,** 1211.

[212] Maschmeyer, T., Oldroyd, R. D., Sankar, G., Thomas, J. M., Shannon, I. J., Klepetko, J. A., Masters, A. F., Beattie, J. K., and Catlow, C. R. A., 1997, *Ang. Chem. int. Ed. Engl.,* **36,** 1639.

[213] Diaz, J. F., Balkus, K. J., Bedioui, F., Kurshev, V., and Kevan, L., 1997, *Chem. Mater.*, **9,** 61.

[214] Liu, C. J., Li, S. G., Pang, W. Q., and Che, C. M., 1997, *J. chem. Soc., chem. Commun.*, 65.

[215] Corma, A., Martinez, A., Martinezsoria, V., and Monton, J. B., 1995, *J. Catal.*, **153,** 25.

[216] Huber, C., Moller, K., and Bein, T., 1994, *J. chem. Soc., chem. Commun.*, 2619.

[217] Pöppl, A., Baglioni, P., and Kevan, L., 1995, *J. phys. Chem.*, **99,** 14 156.

[218] Zhou, H. S., Sasabe, H., and Honma, I., 1998, *J. mater. Chem.*, **3,** 515.

[219] Kozhevnikov, I. V., Sinnema, A., Jansen, R. J. J., Pamin, K., and Vanbekkum, H., 1995, *Catal. Lett.*, **30,** 241.

[220] Kozhevnikov, I. V., Kloetstra, K. R., Sinnema, A., Zandbergen, H. W., and VanBekkum, H., 1996, *J. Mol. Catal. A*, **114,** 287.

[221] Kozhevnikov, I. V., 1998, *Chem. Rev.*, **98,** 171.

[222] Burkett, S. L., Sims, S. D., and Mann, S., 1996, *J. chem. Soc., chem. Commun.*, 1367.

[223] Lim, M. H., Blanford, C. F., and Stein, A., 1997, *J. Am. chem. Soc.*, **117,** 4090.

[224] Macquarrie, D. J., 1996, *J. chem. Soc., chem. Commun.*, 1961.

[225] Macquarrie, D. J., and Jackson, D. B., 1997, *J. chem. Soc., chem. Commun.*, 1781.

[226] Ciesla, U., Demuth, D., Leon, R., Petroff, P., Stucky, G. D., Unger, K., and Schuth, F., 1995, *Stud. surf. Sci. Catal.*, **91,** 337.

[227] Abe, T., Taguchi, A., and Iwamoto, M., 1995, *Chem. Mater.*, **7,** 1429.

[228] Antonelli, D. M., Nakahira, A., and Ying, J. Y., 1996, *Inorg. Chem.*, **35,** 3126.

[229] Antonelli, D. M., and Ying, J. Y., 1996, *Chem. Mater.*, **8,** 874.

[230] Antonelli, D. M., and Ying, J. Y., 1996, *Ang. Chem. int. Ed. Engl.*, **35,** 426.

[231] Antonelli, D. M., and Ying, J. Y., 1995, *Ang. Chem. int. Ed. Engl.*, **34,** 2014.

[232] Stone, V. F., and Davis, R. J., 1998, *Chem. Mater.*, **10,** 1468.

[233] Ulagappan, N., and Rao, C. N. R., 1996, *J. chem. Soc., chem. Commun.*, 1685.

[234] Reddy, J. S., and Sayari, A., 1996, *Catal. Lett.*, **38,** 219.

[235] Ciesla, U., Schacht, S., Stucky, G. D., Unger, K. K., and Schuth, F., 1996, *Ang. Chem. int. Ed. Engl.*, **35,** 541.

[236] Liu, P., Liu, J., and Sayari, A., 1997, *J. chem. Soc., chem. Commun.*, 577.

[237] Doi, T., and Miyake, T., 1996, *J. chem. Soc., chem. Commun.*, 1635.

[238] Tian, Z. R., Tong, W., Wang, J. Y., Duan, N. G., Krishnan, V. V., and Suib, S. L., 1997, *Science*, **276,** 926.

[239] Braun, P. V., Osenar, P., and Stupp, S. I., 1996, *Nature*, **380,** 325.

[240] Attard, G. S., Göltner, C. G., Corker, J. M., Henke, S., and Templer, R. H., 1997, *Ang. Chem. int. Ed. Engl.*, **36,** 1315.

[241] Attard, G. S., Bartlett, P. N., Coleman, N. R. B., Elliott, J. M., Owen, J. R., and Wang, J. H., 1997, *Science*, **278,** 838.

[242] Grun, M., Kurganov, A. A., Schacht, S., Schuth, F., and Unger, K. K., 1996, *J. Chromatogr. A*, **740,** 1.

[243] Mercier, L., and Pinnavaia, T. J., 1997, *Adv. Mater.*, **9,** 500.

[244] Corma, A., Fornes, V., Garcia, H., Miranda, M. A., and Sabater, M. J., 1994, *J. Am. chem. Soc.*, **116,** 9767.

[245] Abe, T., Tachibana, Y., Uematsu, T., and Iwamoto, M., 1995, *J. chem. Soc., chem. Commun.*, 1617.

[246] Tang, Y. S., Cai, S., Jin, G., Duan, J., Wang, K. L., Soyez, H. M., and Dunn, B. S., 1997, *Appl. Phys. Lett.*, **71,** 2448.

[247] Gu, G., Ding, W. P., Du, Y. W., Huang, H. J., and Yang, S. H., 1997, *Appl. Phys. Lett.*, **70,** 2619.

[248] Rachdi, F., Hajji, L., Goze, C., Jones, D. J., Mairelestorres, P., and Roziere, J., 1996, *Solid State Commun.*, **100,** 237.

[249] Wu, C. G., and Bein, T., 1994, *Science*, **264,** 1757.

[250] Wu, C. G., and Bein, T., 1994, *Chem. Mater.*, **6,** 1109.

[251] Wu, C. G., Esnouf, S., and Bein, T., 1993, *Abs. Am. chem. Soc.*, **206,** 142.

[252] Wu, C. G., and Bein, T., 1994, *Science*, **266,** 1013.

[253] Wu, C. G., and Bein, T., 1994, *Stud. surf. Sci. Catal.*, **84,** 2269.

[254] Llewellyn, P. L., Ciesla, U., Decher, H., Stadler, R., Schuth, F., and Unger, K. K., 1994, *Stud. surf. Sci. Catal.*, **84,** 2013.

[255] Blum, Z., and Hyde, S. T., 1994, *Acta chemica Scan.*, **48,** 88.